

Dissertation

Chemical looping for synthesis gas and power generation with CO₂ capture - pilot plant study and process modeling

ausgeführt zum Zwecke der Erlangung des akademischen Grades eines Doktors der technischen Wissenschaften unter der Leitung von

Univ. Prof. Dipl.-Ing. Dr. techn. Hermann Hofbauer
Dipl.-Ing. Dr. techn. Tobias Pröll

E 166
Institut für Verfahrenstechnik, Umwelttechnik und Technische Biowissenschaften der Technischen Universität Wien

eingereicht an der Technischen Universität Wien

Fakultät für Maschinenwesen und Betriebswissenschaften

von
Dipl.-Ing. Johannes Bolhàr-Nordenkampf
Matr. Nr.: 9926085
Beethovengang 10
1190 Wien

Wien, Mai 2009

.....
(Johannes Bolhàr-Nordenkampf)

ABSTRACT

The thesis comprises the experimental investigation of a chemical looping reforming for synthesis gas generation and the implementation of a model library for the description of the chemical looping gas-solid reactors in the simulation software IPSEpro. Additionally a semi-commercial 10 MW_{th} chemical looping combustion plant for power production is proposed as a next scale demonstration plant.

Two different chemical looping process configurations are discussed. The first one, chemical looping autothermal reforming represents a chemical looping system operated at a global air/fuel ratio below one. The second configuration represents a tubular steam reformer utilizing heat from a chemical looping combustor. Further synthesis upgrading steps (shift reactors, CO₂ separation, etc.) are considered for both applications. It can be concluded, that chemical looping systems for synthesis production may be an attractive competitor to standard reforming technology in the near future.

To underline the presented process application operating results of the chemical looping pilot rig at Vienna University of Technology are shown. The reactor system consists of two reactors, an air reactor and a fuel reactor with a suitable oxygen carrier that transports the necessary oxygen for operation. A highly active nickel based oxygen carrier is tested in a novel dual circulating fluidized bed (DCFB) system at a scale of 140 kW fuel power. The mean particle size of the oxygen carrier is 120 μm and the pilot rig is fueled with natural gas. A comprehensive experimental campaign of about 200 h of operation was conducted. The presented data represent the fuel reactor gas concentrations at three different fuel reactor temperatures over a variation of the global air/fuel ratio. For the investigated oxygen carrier high CH₄ conversion is achieved. The observed synthesis gas composition is close to thermodynamic equilibrium. In spite of the fact that no additional steam has been added to the fuel, besides the one present through steam fluidization of the loop seals, coke formation does not occur at global stoichiometric air/fuel ratios above 0.46.

To evaluate the measurements a model library for the description of the chemical looping gas-solid reactors has been created in the equation-oriented IPSEpro environment. The models are based upon conservation of mass and energy and allow the calculation of thermodynamic equilibrium with the thermodynamic data of different metal oxide systems implemented. The model assumptions are made in agreement with operating experience from laboratory installations. The characteristics of the technology are discussed using the presented models for the two fluidized bed reactors. After validation of the modeling tool a semi-commercial 10 MW_{th} chemical looping combustion plant for power production is proposed as a next scale demonstration plant. The design criteria for the chemical looping combustion boiler are derived from the experience at the 140 kW chemical looping pilot rig. A single pressure steam cycle is suggested for the small scale demonstration plant. Heat exchangers and a five-stage steam turbine are arranged. By simulation, design parameters of the power plant are derived and discussed. It turns out that the net electric efficiency of such a small scale plant can be expected to be in the range of 36 %. However, a demonstration of chemical looping combustion at such a scale is necessary in order to gain confidence in more sophisticated CLC power generation concepts at larger scale.

KURZFASSUNG

Bei dem vorgestellten Chemical Looping System handelt es sich um ein Reaktorsystem mit zwei separaten Reaktoren, ein Luftreaktor und ein Brennstoffreaktor, zwischen diesen ein Sauerstoffträger, ein Metalloxid, zirkuliert und somit selektiv Sauerstoff vom Luftreaktor zum Brennstoffreaktor transportiert wird. Im Verbrennungsbetrieb mit Kohlenwasserstoffen entsteht daher ein Abgas aus CO_2 und H_2O ohne die Verdünnung durch Luftstickstoff. Dieser Verbrennungsprozeß gehört zu den potentiellen CO_2 -Abscheidungsmöglichkeiten und wird zur Gruppe der Unmixed Combustion gezählt.

In dieser Arbeit wird das neue Reaktorkonzept Dual Circulating Fluidized Bed (DCFB) kurz vorgestellt, das im Rahmen der Errichtung einer Versuchsanlage an der Technischen Universität Wien entwickelt wurde. Neben der Auswertung und Diskussion der Ergebnisse in der Betriebsart Reformieren, das globale Luft zu Brennstoff Verhältnis ist unter dem stöchiometrischen Verhältnis von 1, wird auch ein detaillierter Versuchsablauf beschrieben. Bei den vorgestellten Ergebnissen wurden ein nickelbasierter Sauerstoffträger und Erdgas als Brennstoff eingesetzt. Die Versuchsanlage wurde über 200 h betrieben. Exemplarisch wird die Gaszusammensetzung bei drei verschiedenen Brennstoffreakortemperaturen und Variation des globalen Luft zu Brennstoff Verhältnis diskutiert. Die thermische Leistung lag für alle Versuchspunkte bei ca. 145 kW. Es konnten, sowohl im Verbrennungsmodus sowie im Reformierungsmodus, hohe CH_4 Umsatzraten erzielt werden. Im Reformierungsbetrieb wurde für fast alle Versuchspunkte das thermodynamische Gleichgewicht erreicht. Eine besondere Erkenntnis aus den Versuchen stellt die nicht vorhandene Koksbildung bis zu einem globalen Luft zu Brennstoff-Verhältnis 0.46 im Reformierungsreaktor dar, obwohl kein zusätzlicher Dampf, außer den Dampf durch die Siphonfluidisierung, dem Brennstoff beigemischt wurde.

Für die Auslegung der Versuchsanlage und für die Evaluierung der Meßergebnisse wurde ein Simulationsmodell des Gas-Feststoffreaktors in der Programmierumgebung des gleichungsorientierten Prozeßsimulationsprogramms IPSEpro entwickelt. Das Modell basiert auf der Einhaltung von Massen- und Energiebilanz mit einer optionalen Berechnung thermodynamischer Gleichgewichte für die integrierten Sauerstoffträgersysteme. Die Validierung des Modells wurde an Hand der Ergebnisse der Versuchsanlage durchgeführt.

Basierend auf das validierte Prozeßsimulationsmodell wurde eine $10 \text{ MW}_{\text{th}}$ Chemical Looping Anlage mit Dampfkraftprozeß gerechnet. Für die veranschlagte Größe des Kessels wurde ein Eindruckdampfkreislauf konzipiert, der mit einer fünfstufigen Dampfturbine verbunden ist. Die Grunddaten des Kraftwerksprozesses wurden berechnet, wobei der netto elektrische Wirkungsgrad der Anlage in der Größenordnung von 36 % liegt. Um diese Technologie voran zu treiben und weiter zu entwickeln ist es von Nöten eine Anlage dieses Maßstabs zu bauen, um ein besseres Verständnis für den doch komplexen Aufbau der Chemical Looping Technologie zu bekommen.

LIST OF PUBLICATIONS

- [I] BOLHAR-NORDENKAMPF, J., PRÖLL, T., KOLBITSCH, P., AND HOFBAUER, H. Comprehensive modeling tool for chemical looping based processes. *Chemical Engineering and Technology* 32, 3 (2009), 410–417.
- [II] BOLHAR-NORDENKAMPF, J., PRÖLL, T., KOLBITSCH, P., AND HOFBAUER, H. Performance of a NiO-based oxygen carrier for chemical looping combustion and reforming in a 120 kW unit. *Energy Procedia* 1, 1 (February 2009), 19–25.
- [III] BOLHAR-NORDENKAMPF, J., PRÖLL, T., KOLBITSCH, P., AND HOFBAUER, H. Chemical looping autothermal reforming at a 120 kW pilot rig. In *Proceedings of the 20th International Conference on Fluidized Bed Combustion Conference* (Xi'an, China, 2009).
- [IV] BOLHAR-NORDENKAMPF, J., PRÖLL, T., KOLBITSCH, P., AND HOFBAUER, H. Chemical looping reforming for syngas generation from natural gas - based on results from a 120 kW fuel power installation. In *accepted for publication in Syngas: Production Methods, Post Treatment and Economics*. Nova Science Publishers, Inc., Hauppauge, NY 11788, USA, 2009.
- [V] BOLHAR-NORDENKAMPF, J., PRÖLL, T., KOLBITSCH, P., AND HOFBAUER, H. Chemical looping combustion for power generation - concept study for a 10 MWth demonstration plant. *submitted to Combustion and Flame* (2009).
- [VI] PRÖLL, T., BOLHAR-NORDENKAMPF, J., KOLBITSCH, P., MARX, K., AND HOFBAUER, H. Pure hydrogen and pure carbon dioxide from gaseous hydrocarbons by chemical looping reforming. In *Proceedings of the 2009 AIChE Spring National Meeting and 5th Global Congress on Process Safety* (Tampa, FL, USA, April 2009).

Contribution by the author:

- [I] Experimental work, data evaluation and writing
- [II] Experimental work, data evaluation and writing
- [III] Experimental work, data evaluation and writing
- [IV] Simulation work, data evaluation and writing
- [V] Simulation work, data evaluation and writing
- [VI] Experimental work, data evaluation

RELATED PUBLICATIONS NOT INCLUDED IN THE THESIS

- [I] KOLBITSCH, P., BOLHAR-NORDENKAMPF, J., PRÖLL, T., AND HOFBAUER, H. Comparison of two Ni-based oxygen carriers for chemical looping combustion of natural gas in 140 kW continuous looping operation. *submitted to Industrial & Engineering Chemistry Research* (2009).
- [II] KOLBITSCH, P., BOLHAR-NORDENKAMPF, J., PRÖLL, T., AND HOFBAUER, H. Design of a chemical looping combustor using a dual circulating fluidized bed (DCFB) reactor system. *Chemical Engineering and Technology* 32, 3 (2009), 398–403.
- [III] KOLBITSCH, P., PRÖLL, T., BOLHAR-NORDENKAMPF, J., AND HOFBAUER, H. Operating experience with chemical looping combustion in a 120 kW dual circulating fluidized bed (DCFB) unit. *accepted for publication in Energy Procedia* (2008).
- [IV] KOLBITSCH, P., PRÖLL, T., BOLHAR-NORDENKAMPF, J., AND HOFBAUER, H. Characterization of chemical looping pilot plant performance via experimental determination of solids conversion. *Energy & Fuels* 23, 3 (2009), 1450–1455.
- [V] PRÖLL, T., KOLBITSCH, P., BOLHAR-NORDENKAMPF, J., AND HOFBAUER, H. A dual circulating fluidized bed (DCFB) system for chemical looping combustion. In *Proceedings of the 2009 AIChE Annual Meeting* (Philadelphia, U.S., 2008).
- [VI] PRÖLL, T., KOLBITSCH, P., BOLHAR-NORDENKAMPF, J., AND HOFBAUER, H. Fluidized bed reactor system. International Application No.: PCT / AT2008/000287, February 2009. Pub. No.: WO/2009/021258.
- [VII] PRÖLL, T., KOLBITSCH, P., BOLHAR-NORDENKAMPF, J., AND HOFBAUER, H. A novel dual circulating fluidized bed (DCFB) system for chemical looping processes. *accepted for publication in AIChE Journal* (2009).
- [VIII] PRÖLL, T., MAYER, K., BOLHAR-NORDENKAMPF, J., KOLBITSCH, P., MATTISSON, T., LYNGFELT, A., AND HOFBAUER, H. Natural minerals as oxygen carriers for chemical looping combustion in a dual circulating fluidized bed system. *accepted for publication in Energy Procedia* (2008).
- [IX] PRÖLL, T., RUPANOVITS, K., KOLBITSCH, P., BOLHAR-NORDENKAMPF, J., AND HOFBAUER, H. Cold flow model study on a dual circulating fluidized bed (DCFB) system for chemical looping processes. *Chemical Engineering and Technology* 32, 3 (2009), 418–424.

ACKNOWLEDGMENT

I would like to thank the following people for helping me with the work for this thesis or supporting me in stressful times.

First of all, I would like to thank Univ.-Prof. Dr. Hermann Hofbauer for giving me the opportunity to work at the Institute of Chemical Engineering.

My supervisor Dr. Tobias Pröll for the excellent supervision of my work and for all valuable discussions on chemical looping or other topics.

My CLC colleague Philipp Kolbitsch for the enjoyable team-work in the office and in the technical lab and for many fruitful discussions in the last three and half years.

All of my colleagues in the research group for the pleasant working atmosphere.

My brother Markus who motivated me in stressful times.

A special thank to Maren for her endless support everyday over the last years and her willingness to motivate me consistently.

TABLE OF CONTENTS

1	INTRODUCTION	1
1.1	CLIMATE CHANGE	1
1.2	CARBON CAPTURE AND STORAGE.....	5
1.3	AIM OF THIS WORK.....	8
2	THE CHEMICAL LOOPING SYSTEM	9
2.1	PRINCIPLE OF CHEMICAL LOOPING COMBUSTION.....	9
2.2	SYNTHESIS GAS PRODUCTION WITH CHEMICAL LOOPING	12
2.2.1	CHEMICAL LOOPING AUTOTHERMAL REFORMING FOR H ₂ PRODUCTION	13
2.2.2	CHEMICAL LOOPING COMBUSTION STEAM REFORMING	15
2.3	OXYGEN CARRIER	17
2.4	REACTOR SYSTEMS FOR CHEMICAL LOOPING PROCESSES	19
2.4.1	DUAL CIRCULATING FLUIDIZED BED SYSTEM.....	21
3	EXPERIMENTAL	23
3.1	THE 120 KW DCFB PILOT RIG	23
3.1.1	ARRANGEMENT IN THE LABORATORY.....	25
3.1.2	AUXILIARY EQUIPMENT.....	25
3.1.3	GAUGE POINTS	26
3.2	EXPERIMENTAL CAMPAIGN.....	27
3.2.1	EXPERIMENT PREPARATION.....	27
3.2.2	START UP PROCEDURE.....	27
3.2.3	CHEMICAL LOOPING OPERATION.....	28
3.2.4	SHUT DOWN PROCEDURE	28
3.2.5	ONLINE DATA ACQUISITION SYSTEM.....	28
3.2.6	SOLIDS SAMPLING.....	28
3.2.7	EXPERIMENTAL EVALUATION	29
3.3	HEALTH SAFETY AND ENVIRONMENT ANALYSIS	30

4	PROCESS MODELING AND SIMULATION	31
4.1	THE SIMULATION SOFTWARE IPSEPRO	31
4.2	CHEMICAL LOOPING SIMULATION MODEL	31
4.2.1	SUBSTANCE CLASSES AND THERMODYNAMIC PROPERTIES.....	31
4.2.2	THERMODYNAMIC EQUILIBRIUM FORMULATION.....	32
4.2.3	REDOX SYSTEMS AND REACTIONS MODELED.....	32
4.2.4	SIMULATION FLOW SHEET OF THE CLC PROCESS.....	34
4.2.5	RECONCILIATION OF DATA DERIVED PARAMETERS	34
5	RESULTS FROM 120 KW PILOT PLANT	38
5.1	CLC EXPERIMENTAL RESULTS.....	38
5.2	CLR EXPERIMENTAL CAMPAIGN.....	40
6	A 10 MW_{TH} CLC CONCEPT	45
7	CONCLUSION	53
8	NOTATION	55
9	REFERENCES	57

1

INTRODUCTION

1.1 CLIMATE CHANGE

The Intergovernmental Panel on Climate Changes defines climate change as

the change in the state of climate that can be identified by changes in the mean and/or the variability of its properties, and that persists for an extended period, typically decades or longer. It refers to any change in climate over time, whether due to natural variability or as a result of human activity. [20]

Climate changes can be observed all over the world by increasing global average surface temperature and increase global average sea level (see Fig. 1). Regional effects can be seen especially at higher northern latitude. Glacier decrease in size and glacial lakes enlarge or emerge. Permafrost areas in the mountains and in Siberia decrease which results in an increasing ground instability. Changes in the Arctic and Antarctic ecosystem make it impossible for some animals to survive.

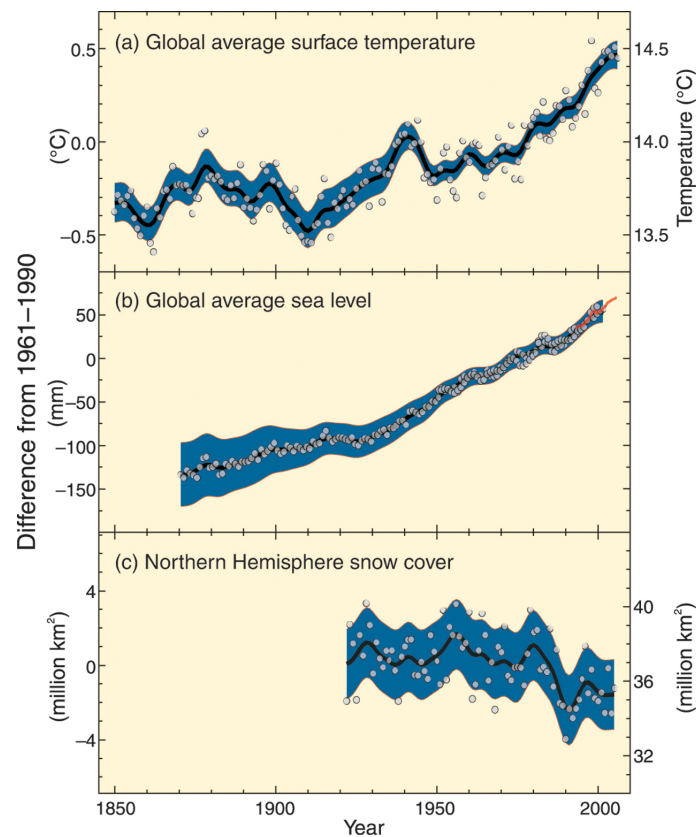


Fig. 1 Temperature and sea level increase and snow cover decrease [20]

The drivers of climate change are the atmospheric concentrations of green house gases GHGs, aerosols, land cover and solar radiation. They affect the energy balance of the climate system by means of absorption, scattering and emission of radiation within the atmosphere and at the Earth's surface. Fig. 2 gives a simplified schema of the energy balance on Earth.

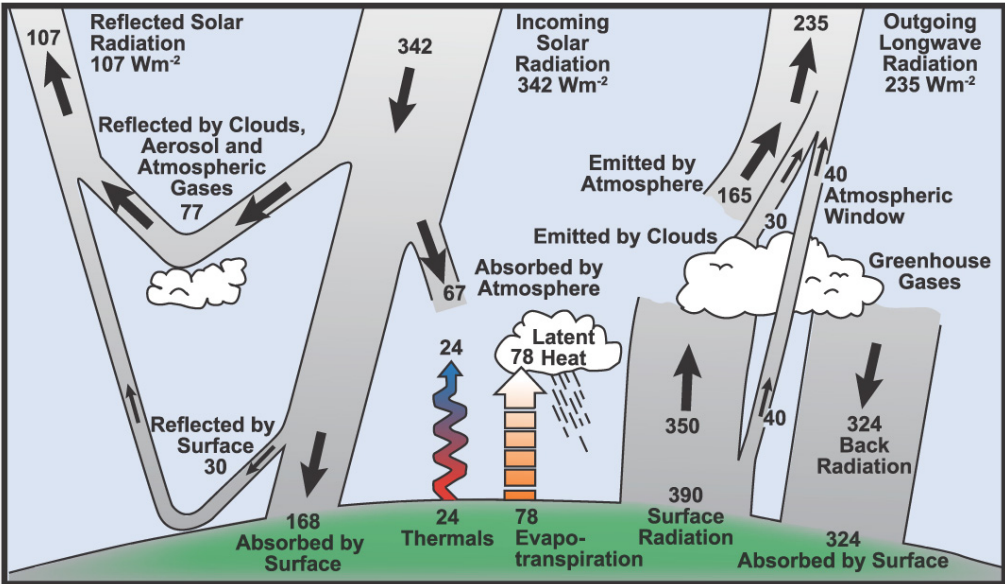


Fig. 2 Energy balance on Earth [20]

The anthropogenic influence on the climate summarizes in:

- Emissions of long-lived GHGs (CO₂, N₂O, CH₄, halocarbon),
- Emission of aerosols,
- Emission of ozone and
- Influence on the surface albedo.

IPCC concludes that the increase of GHGs by human activities represents the major driver for most observed temperature increase [20]. There has been a steady increase in GHGs in the last 100 years (see Fig. 3). To better understand and to compare different GHGs and their impact on the climate, the value of CO₂-equivalent emission is defined as

the amount of CO₂ emission that would cause the same time-integrated radiative forcing, over a given time horizon (e.g. 100years), as an emitted amount of a long-lived GHG or a mixture of GHGs. The equivalent CO₂ emission is obtained by multiplying the emission of a GHG by its Global Warming Potential for the given time horizon. For a mix of GHGs it is obtained by summing the equivalent CO₂ emissions of each gas. Equivalent CO₂ emission is a standard and useful metric for comparing emissions of different GHGs but does not imply the same climate change responses. [20]

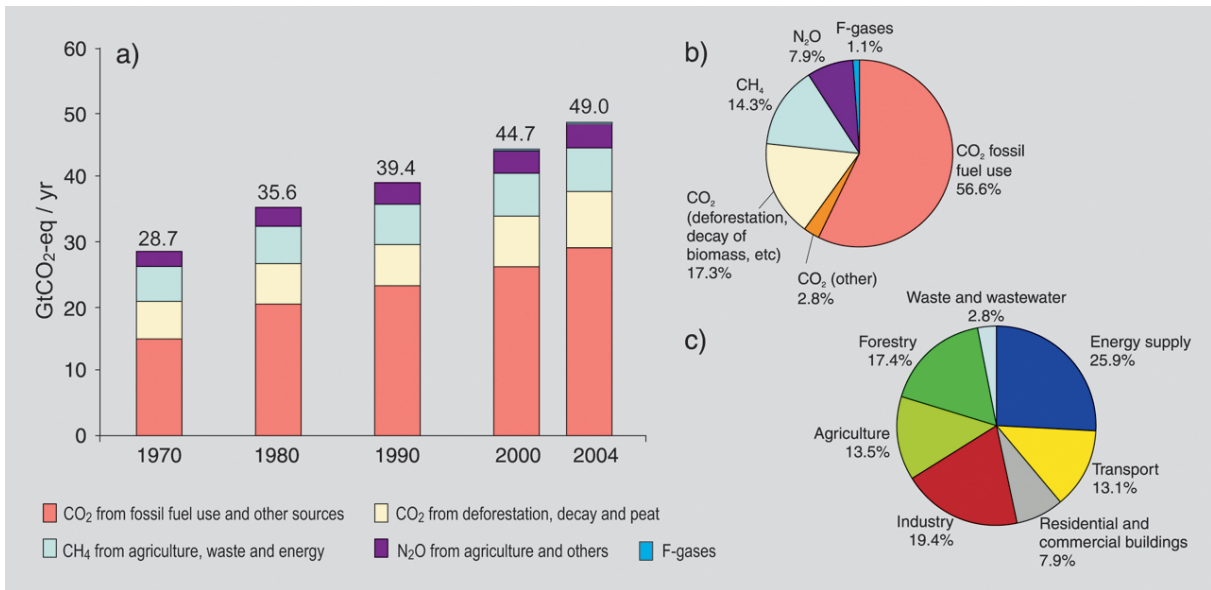


Fig. 3 a) Global annual emissions of anthropogenic GHGs from 1970 to 2004
 b) Share of different anthropogenic GHGs in total emissions in 2004 in terms of CO₂-eq.
 c) Share of different sectors in total anthropogenic GHG emissions in 2004 in terms of CO₂-eq.
 F-gases are fluoride containing gases (e.g. hydrofluorocarbons, perfluorocarbons, etc.) [20]

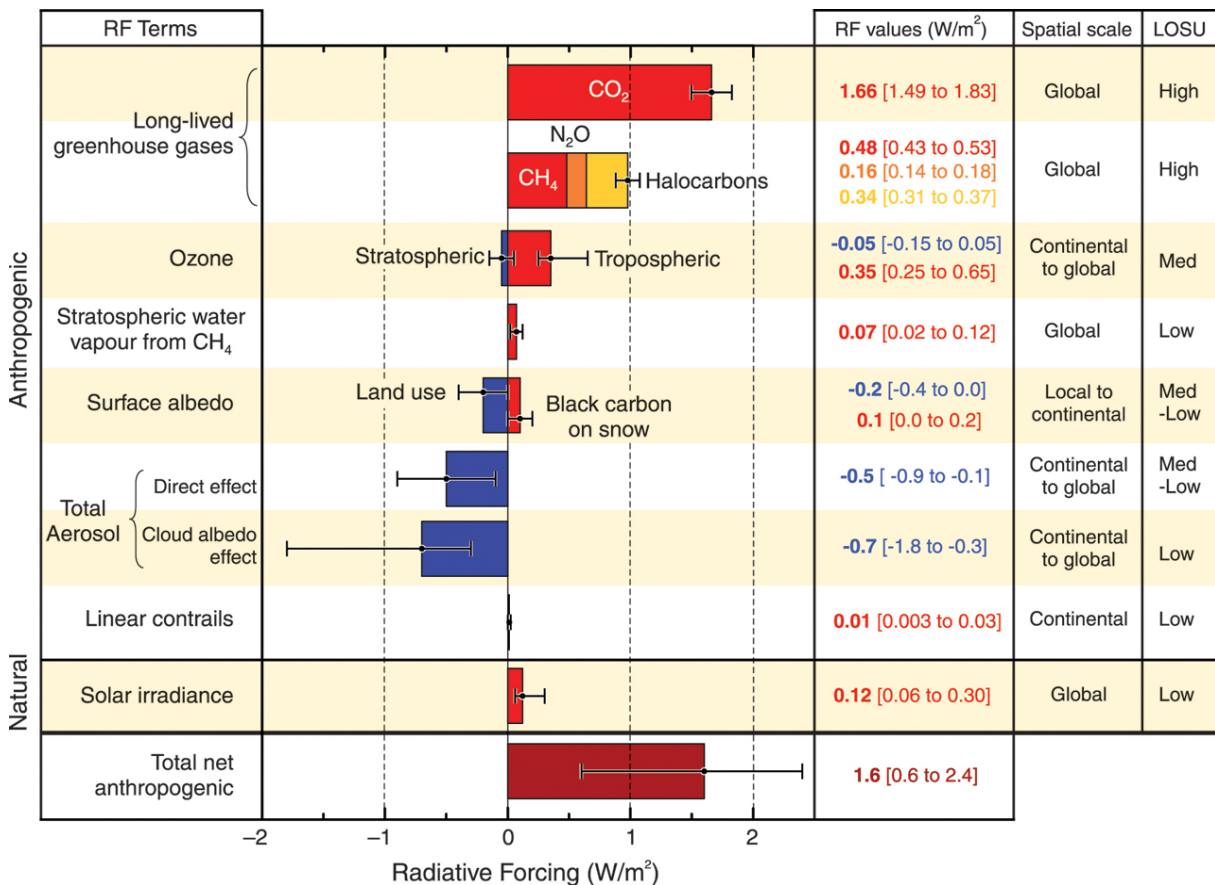


Fig. 4 Radiative forcing (RF) of the year 2005 compared to 1750 (level of scientific understanding LOSU) [20]

The radiative forcing, as defined by the IPCC, describes the difference between the incoming radiation energy and the outgoing radiation energy in a given climate system compared to the beginning of the industrial era in the year 1750. The radiative forcing is measured in Watts per square meter. Due to radiative forcing of different compounds in the atmosphere and factors on the Earth's surface the planet's climate is warmer than it would be in the absence of those. Fig. 4 gives a summary of all anthropogenic and natural components affecting the radiative forcing for the year 2005. It can be concluded that the long-lived GHGs have a major impact on the increase compared to the year 1750. It's very likely that anthropogenic CO₂ emissions contribute to global warming therefore strategies to reduce those emissions are necessary.

Different mitigation options to achieve GHG emission reduction are discussed by IPCC [20] and the UNFCCC.

- Energy efficiency improvement,
- The switch to less carbon-intensive fuels,
- Nuclear power,
- Renewable energy sources,
- Enhancement of biological sinks,
- Reduction of non CO₂ GHG emissions,
- CO₂ capture and storage (CCS).

In practice, only a portfolio of all the options will make the goal of reducing the GHGs achievable. Since CO₂ emissions play a major role, CCS technologies have a great potential to reduce overall mitigation costs and increase flexibility in achieving GHG short term emission reduction [20].

1.2 CARBON CAPTURE AND STORAGE

The basic scenario for CCS focuses on large point sources of CO₂, independently of the primary energy source used. In other words, any CO₂ not emitted to the atmosphere, even from renewable energy sources (e.g. biomass), contributes to the reduction of GHGs. In Table 1 an overview of the world wide largest stationary CO₂ sources is shown. [20]

Table 1 Worldwide large stationary CO₂ sources (2005) [20]

Process	Number of sources	Emissions [MtCO ₂ /yr]
Fossil fuels		
Power production	4 942	10 539
Cement production	1 175	932
Refineries	638	798
Iron and steel industry	269	646
Petrochemical industry	470	379
Oil and gas processing	not available	50
other sources	90	33
Bio ethanol and bio energy	303	91
Total	7 887	13 466

Fossil fuels represent the largest emission source and within this share the power production sector contributes most CO₂ emissions. Policymakers have to make the way clear for implementation of innovative technologies by stating legal frameworks and basic conditions. The first global incentives for local governments to act were given by the Kyoto Protocol in the year 1992. It represents an outcome of the United Nation Conference on Environment and Development and intends to achieve *“stabilization of the greenhouse gas concentration in the atmosphere at a level that would prevent dangerous anthropogenic interference with the climate system”* [57]. In 2002 all fifteen then-members of the European Union ratified the Kyoto Protocol and in 2007 the European Commission announced plans for reducing the GHG emissions by 20% in the year 2020. One recent outcome, especially important for the European Union, was the agreement of the German Ministry for Economy and the Ministry of Environment on a law on carbon storage [56]. Germany, as an important member of the European Union and a leading player in the European Economy will hopefully influence other member countries to start rethinking the topic of CCS.

Carbon capture technologies require energy for capture, transport and storage. Therefore, a power plant with CCS technology will consume, depending of the type of plant roughly 10 – 40% more primary energy than a plant of equivalent output without CCS [19]. Additionally, the technologies available today cannot capture 100% of the CO₂ emitted from a plant. Common capture rates lie in a range of 85 – 95%. These two drawbacks have to be taken into account when comparing the

different capture technologies. This correlation can be expressed by the CO₂ avoidance rate and the CO₂ capture rate of a CCS technology (see Fig. 5).

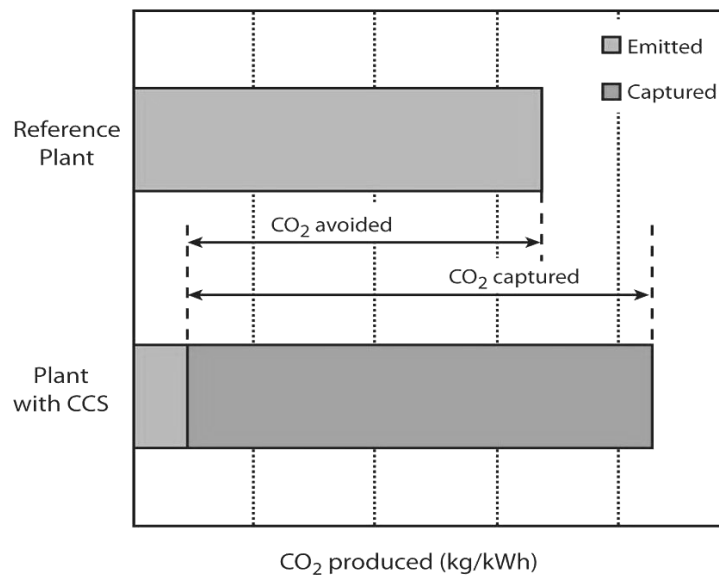


Fig. 5 CO₂ avoidance rate and CO₂ capture rate

There are different types of CO₂ capture systems which all have the same aim producing a dry CO₂ stream for transport and storage. A CO₂ stream containing moisture would lead to corrosion in the pipelines. Different constraints, like the CO₂ concentration in the gas stream and the pressure make different capture technologies feasible for different CO₂ sources.

Post combustion capture, an end of pipe technology, is the farthest developed technology. It is already used as carbon capture technology at existing power plants [19].

A second approach is the *pre-combustion capture* which is widely applied in fertilizer manufacturing and in hydrogen production. In this technology the initial fuel is converted in a pre-combustion step to a synthesis gas and via the shift reaction to H₂ and CO₂. This step is more elaborate and, therefore, costly but the CO₂ separation becomes easier compared to post combustion as the CO₂ concentration and pressure of the synthesis gas is high.

A third option, *oxyfuel combustion*, uses pure oxygen from air separation with recycled flue gas for combustion. In this process the flue gas consists ideally of CO₂ and steam, hence, the separation of CO₂ becomes easier. The major drawback with this technology represents the energy requirement for air separation to gain pure oxygen. Oxyfuel combustion has been demonstrated in a 30 MW plant but needs further development to be ready for full scale systems [58].

A fourth route for carbon capture represents *unmixed combustion* [37]. The aim of this process is a flue gas with high CO₂ concentration similar to oxyfuel combustion. Therefore, air and fuel is never mixed during combustion. To provide the necessary oxygen for combustion of the fuel a selective oxygen transport between air and fuel is needed. Chemical looping combustion represents such a

technology. A pure CO₂ stream is obtained and 100% CO₂ is captured. Ideally the energy penalty for CO₂ separation compared to the other three technologies is zero. This represents the major advantage of this technology but the feasibility has to be proven at full scale as the process is in the stage of research development.

After the CO₂ separation the gas has to be transported to the different storage options. For large-scale sources the most attractive option is the transport in pipelines. This has already been demonstrated in the USA. A pipeline network over 2500 km exists which transports 40 MtCO₂/yr. Some energy penalty has to be taken into account for transportation as a driving force is needed for the flow. Under special conditions (small scale, ocean transport, demonstration, etc.) other transport options like shipping, road tankers or transportation by rail could be feasible [19]. Fig. 6 shows the schematic CCS chain from source to sink.

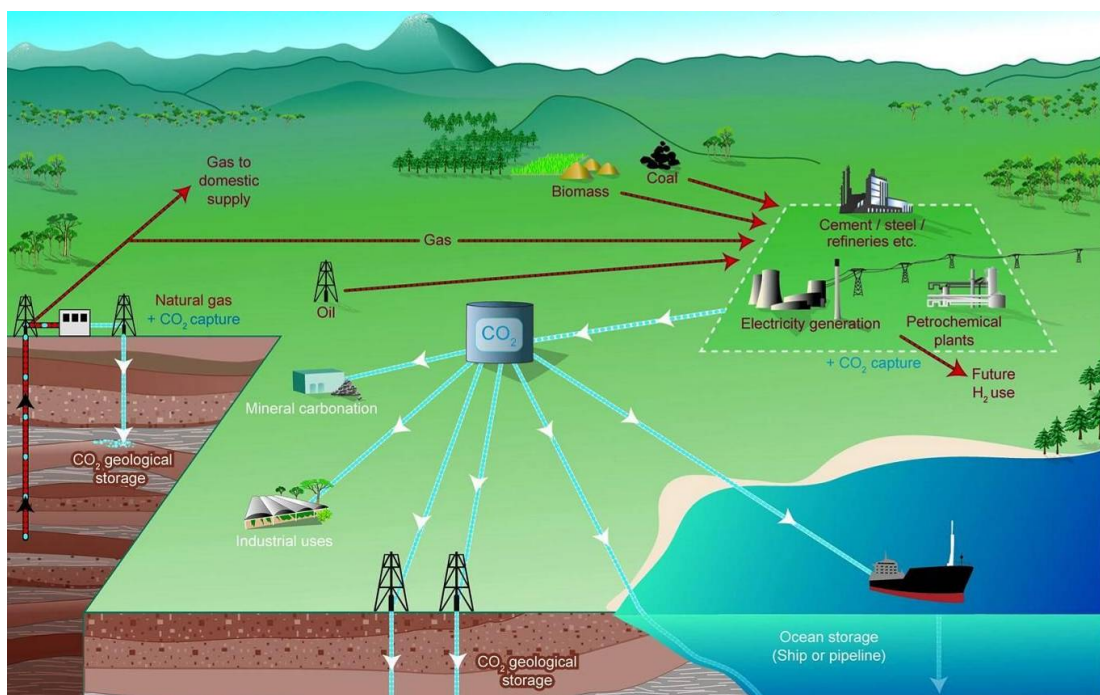


Fig. 6 Schematic diagram of CSS systems (sources, transport and storage of CO₂) [19]

The final step in the chain of CCS represents the storage of CO₂. In general there are four different options: geological storage, ocean storage, production of stable carbonates and use in industrial processes as a feedstock. The technologies are all in different stages of development.

Storage in deep geological formations has been developed by the oil and gas industry and is used for enhanced oil or gas recovery (EOR or EGR). A new field represents the storage in unminable coal beds which could lead to additional revenues from enhanced coal bed methane recovery (ECBM). In the year 2007 the storage technology is already demonstrated in four industrial-scale projects: the Sleipner project in an offshore saline formation in Norway, the project at the Snøhvit gas field in the Barents Sea, the Weyburn EOR project in the USA and in Canada and the In Salah project in Algeria [19].

There are two ways of storing CO₂ in the ocean: by injecting CO₂ into the water and dissolving it or by injecting the CO₂ in a depth below 3000 m, where CO₂ is denser than water. It is expected to form a lake at the sea floor that delays the dissolution of the CO₂ into the surrounding environment. Ocean storage is the most criticized type of CO₂ storage as its ecological impacts are not yet fully understood [19].

The process of formation of carbonates is a natural process. To enhance the reaction special pretreated metal oxides and silicate minerals have to be used. The pretreatment needs additional energy. In the year 2005 this technology was still in the research state.

The use of CO₂ in industrial processes seems to have only small potential as the net lifecycle emission by subsidizing fossil hydrocarbons are not always reduced.

1.3 AIM OF THIS WORK

The research presented in this thesis focuses on the analysis of operating experience of a 120 kW chemical looping pilot rig designed and built at Vienna University of Technology. In the first part of the thesis the chemical looping system for synthesis gas production is introduced. Two possible synthesis gas production configurations are discussed. This content is based on Paper IV and VI.

The second part of this work focuses on the experimental results of the chemical looping pilot rig. To suit the requirements of chemical looping systems a novel reactor design was developed. Additionally, auxiliary units had to be dimensioned and designed for the needs of a pilot plant scale configuration. Furthermore, a complex gas sampling and gas cleaning configuration was built for tar free flue gas analysis. Special requirements in a circulating fluidized bed made it necessary to adapt the pressure measurement for reproducible measurements. After design and erection phase of two years the cold and hot commissioning started late 2007. To gain operating experience on the novel chemical looping reactor system first tests of about 230 h were done with a nonhazardous natural ore (ilmenite). After some modification on the pilot rig for reliable and safe operation a comprehensive experimental campaign for the desired Ni-based particles of about 200 h of operation in 14 experimental days was conducted. This part in the thesis is based on paper II and III.

A process simulation model of the chemical looping reactor was developed in the simulation environment IPSEpro and the whole pilot plant configuration was simulated. Due to the relative novelty of the chemical looping based processes, solid streams and gas-solid reactions had to be implemented in a new model library called advanced energy technology library (AET-Lib). To increase the reproducibility and the accuracy the method of data reconciliation was established. The content of this part is based on Paper I.

Furthermore a concept calculation of a 10 MW_{th} chemical looping combustion boiler for power production is presented. It summarizes the basic design parameters for a next scale demonstration plant and defines operating parameters at nominal load. The results are based on Paper V.

2

THE CHEMICAL LOOPING SYSTEM

2.1 PRINCIPLE OF CHEMICAL LOOPING COMBUSTION

Chemical looping (CL) using metal oxides for selective transport of oxygen is a novel fuel conversion technology. The technology was first proposed in several patent applications by Standard Oil Development Company in the early 1950-ies (e.g. [31]) then proposed by Richter and Knoche [49] to increase the reversibility of combustion processes and in the nineties Ishida et al. [22] proposed it as a possibility to capture CO_2 from fossil fuel. More recently, CL systems based on circulating fluidized beds have been presented as a promising technology for carbon capture from power plants [21, 35, 52].

Chemical looping systems consist of two reaction zones in which different gas streams are in contact with circulating solids. The circulating solids transport oxygen and heat from one reaction zone to the other. These solids will be referred to as oxygen carrier. Several metal oxides allow such a selective oxygen transport. In the fuel converting zone, fuel is oxidized in contact with the oxygen carrier. This reaction zone is called fuel reactor (FR). In the second zone, called air reactor (AR), the oxygen carrier is re-oxidized with air. Fig. 7 shows a basic setup of chemical looping system.

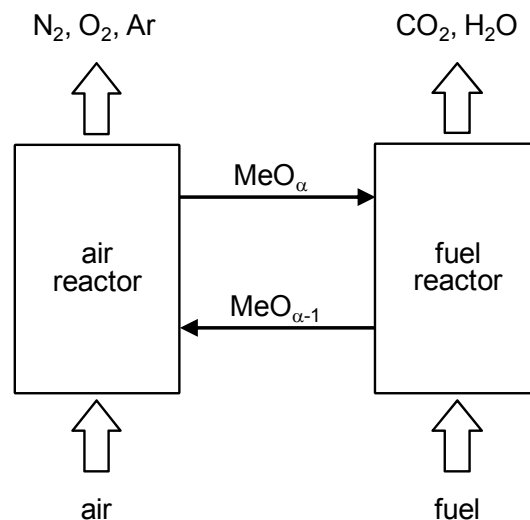
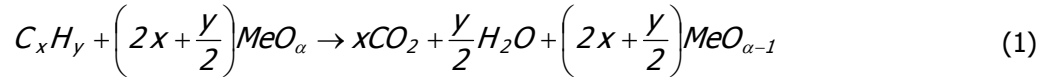


Fig. 7 Basic chemical looping system (e.g. chemical looping combustion)

To characterize the operation mode of a chemical looping system the global air/fuel ratio is defined as the ratio of air to the AR and the air needed for full combustion of the fuel introduced to the FR. In the following, a chemical looping system operated at a global air/fuel ratio above 1 is referred to as

chemical looping combustion (CLC) and operation at a global air/fuel ratio below 1 is called chemical looping reforming (CLR).

In CLC operation, the fuel introduced to the FR reacts with the MeO_α according to:



Ideally the exiting gas stream of the FR consist of CO_2 and H_2O . After condensation a pure CO_2 stream is obtained. The reduced metal oxide $MeO_{\alpha-1}$ is transferred to the AR where it is oxidized.



The AR off gas consists ideally of N_2 , Ar and unused O_2 .

The oxidation and reduction of the metal oxides are gas–solid reactions. To gain best conditions for such reactions some criteria must be considered:

- Enough residence time of particle and gas in the reaction zones,
- Even gas and solid distribution and
- An adequate metal oxide for the fuel used.

These criteria and the necessity of oxygen carrier transport between two reaction zones limit the possible types of reactor systems and the type of particles with respect to design and composition.

The heat release in the two reactors depends on the fuel and the oxygen carrier used. In general the AR reaction is always exothermic whereas the FR reactions can be either endothermic or exothermic. In Fig. 8 the reaction enthalpies for some possible metal oxides with CH_4 are shown. Full oxidation to CO_2 and H_2O is assumed in the FR and in the AR oxidation with O_2 . For the Fe_2O_3/Fe_3O_4 and for the NiO/Ni system, the oxidation is strongly exothermic whereas the reduction with CH_4 is slightly endothermic. For the CuO/Cu system, the FR reaction is slightly exothermic. The dashed line represents the standard enthalpy change of the direct combustion of methane with air. In the ideal case of CLC the overall heat which is produced in both reactors equals to the heat produced in conventional combustion.

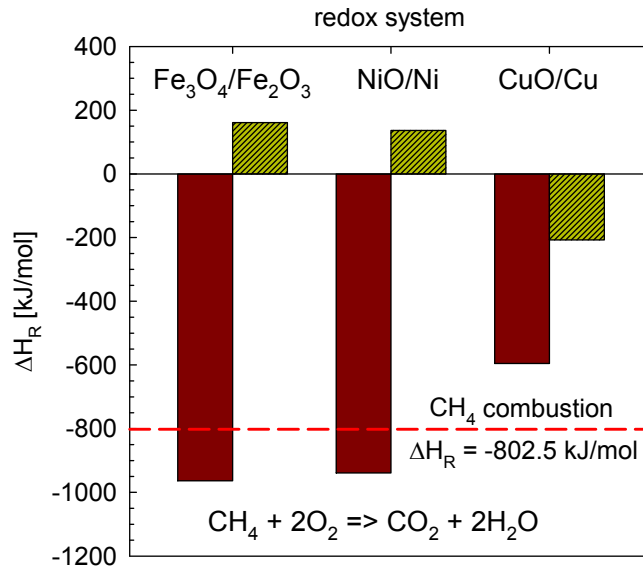


Fig. 8 Enthalpy change of reaction (reduction and oxidation of three metal oxides at 900°C)

Fig. 9 shows the energy balance for CLC and CLR operation. In order to keep the operating temperature at a certain global air/fuel ratio, heat must be withdrawn directly from the reactor system. The necessary reactor cooling reaches the theoretical maximum at global air/fuel ratio of 1. Up to 60% of the total heat release from the reactor system has to be withdrawn by cooling. This can be done either by reactor wall cooling or by bed material cooling with a fluidized bed heat exchanger.

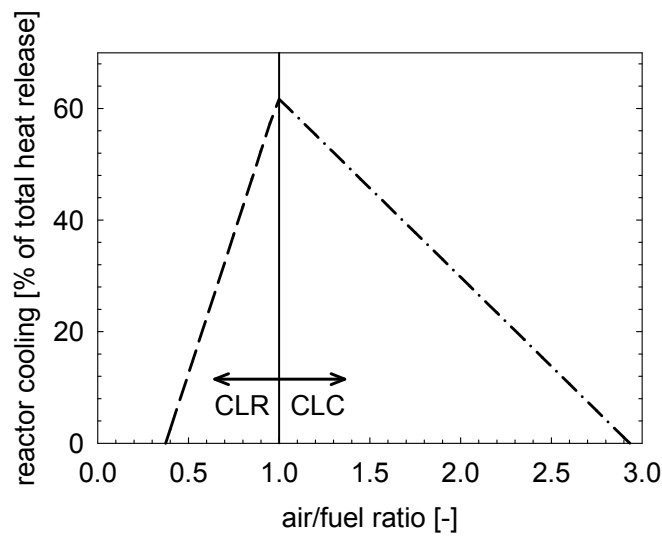
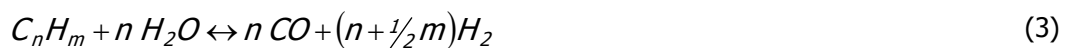


Fig. 9 Heat release of the reactor system (fuel: CH₄, full conversion to equilibrium, T_{FR}=850°C.).

2.2 SYNTHESIS GAS PRODUCTION WITH CHEMICAL LOOPING

The importance of synthesis gas throughout history started as early as the 19th century when so called town gas, a low calorific gas, was produced from coal devolatilization. In 2004 the total global annual use of fossil-derived synthesis gas was approximately 2% of the total primary energy consumption. The main share of the synthesis gas production is used for the synthesis of ammonia for fertilizer production. Other applications where synthesis gas is used are oil refining processes, which use hydrogen from synthesis gas, and methanol production [59]. All kind of hydrocarbon fuels can be used for synthesis gas production, but natural gas is the most important one. The three major reactions for hydrocarbon reforming are:

Steam reforming (endothermic)



CO₂ reforming (endothermic)



Partial oxidation (exothermic)



Additional with those reactions the exothermic water gas shift reaction takes place.



Ideally, the gas composition at the end of the reformer reaches water gas shift and methane steam reforming equilibrium according to the conditions at the exit of the reformer. To increase the yield of H₂ after reforming additional shift reactors at lower temperatures can be arranged to change the composition of the synthesis gas to higher H₂/CO ratios. Once the H₂/CO ratio fits, a CO₂ separation and water condensation step has to be considered. Furthermore, the energy balance of the appearing reactions in the process has to be fulfilled. Steam and CO₂ reforming are highly endothermic whereas partial oxidation and the water gas shift reaction are slightly exothermic. Different process arrangements are possible to introduce the necessary heat to the reforming reaction zones. An autothermal configuration combines endothermic and exothermic reactions in one reaction zone, i.e. it is a thermo-neutral process. On the other hand the energy for endothermic reactions can be provided indirectly, e.g. tubular steam reforming with direct firing.

All mentioned reactions, depending on the configuration of the process, are supported by a catalyst. For the most important synthesis gas generation process today, the tubular steam reforming of natural gas, an Ni-based catalyst is used [12]. The shift reaction can be utilized by an iron/chrome based catalyst.

2.2.1 CHEMICAL LOOPING AUTOTHERMAL REFORMING FOR H₂ PRODUCTION

Chemical looping reforming (CLR) represents a CL system operated at a global air/fuel ratio below the stoichiometric ratio of 1. The autothermal operating point of the CL system is reached where the sensible heat produced in the AR matches the heat requirement of the endothermic reactions in the FR, that is neither cooling nor external heating of the reactor system is needed. The principle of chemical looping reforming is illustrated in Fig. 10.

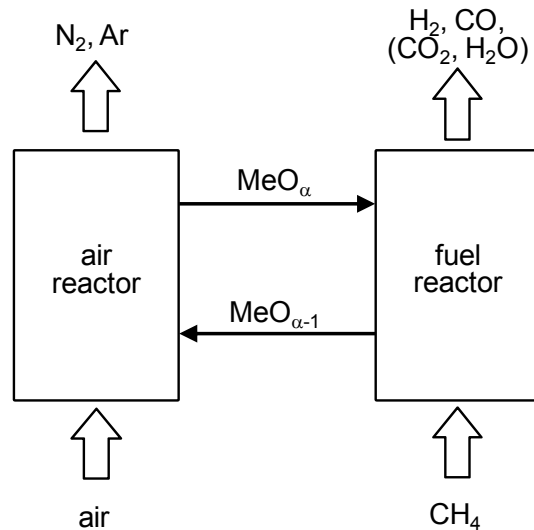


Fig. 10 Schematic description of chemical looping reforming with CH₄ as fuel

In the AR the metal oxide will be oxidized by air via reaction (2). As mentioned above, this reaction is always strongly exothermic. The produced heat in the AR is on the one hand released by the exhaust gas, consisting mainly of N₂ and Ar, on the other hand, by the bed material. The hot bed material transports both oxygen and sensible heat to the FR to utilize the endothermic reaction of fuel reforming and partial oxidation. Different operating parameters, global air/fuel ratio, oxygen carrier and fuel, influence the amount of sensible heat actually needed in the FR. The reduced oxygen carrier leaves the FR at a lower temperature and is heated up again by oxidation in the AR.

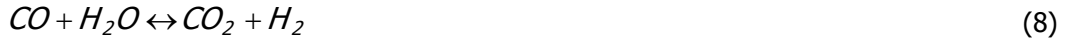
Different exothermic and endothermic reactions take place in the FR at the same time:

- Partial oxidation of the fuel in contact with the oxygen carrier,
- Oxidation of H₂ and CO in contact with the oxygen carrier.
- Steam reforming (with steam present in the FR), CO₂ reforming

If the fuel is methane the main reactions in the FR are:

Steam reforming and water gas shift reaction:





Partial oxidation with NiO:



Internal combustion:



The produced synthesis gas can be upgraded towards higher H_2/CO ratios by a shifting step in a high, middle or low temperature shift reactor. This is especially necessary for production of pure hydrogen. The final upgrading of the synthesis gas includes CO_2 separation and water condensation.

A CLR system with CO_2 separation for production of pure hydrogen is presented in Fig. 11. This process configuration was originally proposed by Rydén and Lyngfelt [50]. The basic process configuration shown in Fig. 11 does not show heat exchangers or the combined cycle equipment for power production.

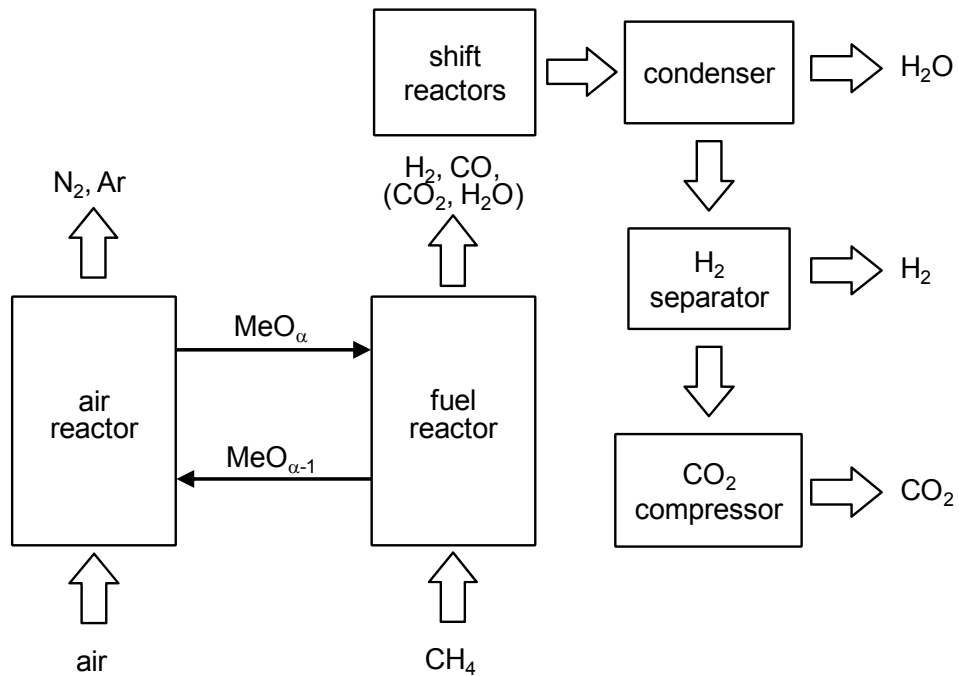


Fig. 11 CLR for hydrogen production

The CLR system is fueled with methane and the obtained synthesis gas is shifted via a high and low temperature shift towards high H₂ concentrations. After condensation of the water the hydrogen is separated from the CO₂ and any other impurities. The hydrogen is then used in a combined cycle as fuel or as starting product in other processes. The CO₂ is compressed and ready for storage. Ideally no off gas is produced and all carbon is captured, however the actual plant will have losses of carbon. The nearly pure nitrogen stream from the AR is used as diluting agent in the hydrogen combustion turbine or as a source for Ar and N₂. It is important to notice that the CLR system is operated at atmospheric pressure, which results in an additional compression step for the hydrogen before it can be used in the combined cycle as well as the nitrogen from the AR. Those two compression steps and the resulting energy consumption represent the main drawback compared to standard pressurized tubular steam reforming. To overcome the efficiency penalty of compressing H₂ and N₂ a pressurized fluidized bed concept could be considered [50]. Other possible process configurations of CLR with synthesis gas upgrading steps seem feasible, which allow a new evaluation of the atmospheric reforming process [42].

2.2.2 CHEMICAL LOOPING COMBUSTION STEAM REFORMING

Chemical looping combustion steam reforming (CLC-SR) uses a CL system operated in combustion mode to supply a tubular steam reformer with heat. The tubular steam reformer is conceived as a fluidized bed heat exchanger (fluidized bed heated steam reformer, FBH-StR). The chemical looping unit with an FBH-StR is shown in Fig. 12. In the fluidized bed tubular steam reformer the heat is transferred from the bed material to the reformer tubes.

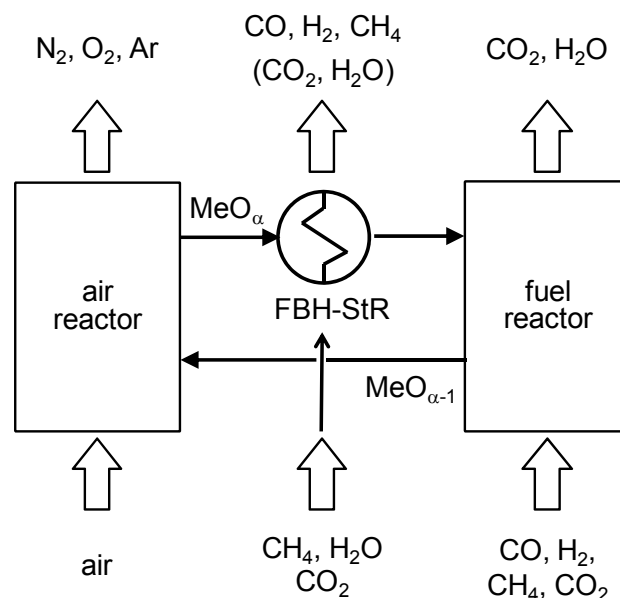


Fig. 12 Chemical looping combustion steam reforming (CLC unit with FBH-StR)

As shown in Fig. 9 the heat withdrawn from the bed material can be up to 60% of the thermal input in the CLC system depending on the operating parameters. Traditionally, the reformer is operated at

elevated pressure and high steam/carbon ratio to avoid carbon formation. Developments of new highly active steam reforming catalysts make it possible to reduce the steam/carbon ratio below 1 with low risk of carbon formation. The reformer off-gas composition is strongly influenced by the pressure, temperature and steam/carbon ratio. In general, an increase in pressure results in a higher equilibrium CH_4 concentration. Increasing the temperature can compensate this effect again [12]. Due to the new developments in the field of reformer catalysts the operating parameters of the reformer can be more easily chosen in favor of the post reformer configuration and the desired end product.

The investigated concept, shown in Fig. 13, represents a CLC-SR process configuration for hydrogen production. Such a configuration again was first proposed by Rydén and Lyngfelt [51]. It combines a CLC-SR system, as described above, with a shift reactor, water condensation and hydrogen separation. The off-gas of the H_2 separation unit (e.g. PSA) consists of CO , unreformed CH_4 , CO_2 and H_2 . It represents the fuel to the FR in CLC system. According to the energy balance of this configuration a dependency between thermal input to the FR and thermal output to the FBH-StR is given. This dependency can be overcome by adding additional fuel to the off-gas of the H_2 separation unit.

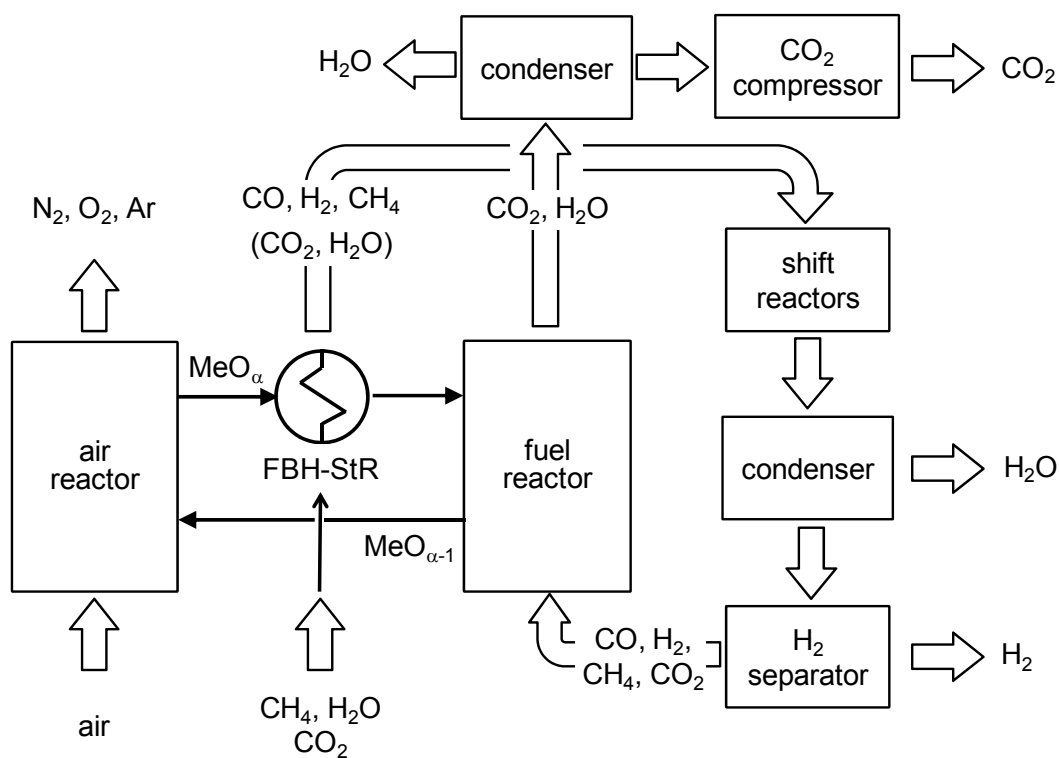


Fig. 13 CH_4 fueled CLC-SR for hydrogen production

The exhaust gas of the FR ideally consists of CO_2 and H_2O and after condensation of the water the CO_2 is ready for compression.

It is beneficial in CLC-SR that, compared to CLR, the produced hydrogen occurs at elevated pressure. Therefore, the apparatus become smaller which results in lower investment costs. The synthesis

upgrading steps represent well known technologies which make such a configuration feasible. The biggest challenge in this concept represents the FBH-StR as such a unit has never been built before. In general, the steam reformer tube design and length determine the size of the FBH-StR in accordance with the bubbling fluidized bed hydrodynamics of fluidized bed heat exchangers. It seems reasonable to believe that these difficulties and others could be contained as fluidized bed heat exchangers are rather conventional technology in circulating fluidized bed boilers [7].

To determine mass and energy balances of such configurations the simulation software IPSEpro is used. Detailed process configurations of CLR and CLC-SR systems are under investigation. Heat integration between the process units and a steam cycle will be implemented, which allow efficiency analysis and determination of basic design parameters. More details can be found in the master thesis of Klemens Marx [38].

2.3 OXYGEN CARRIER

The basic requirements for oxygen carriers (OCs) are thermodynamic suitability, high oxygen transport capacity, high reactivity, mechanical stability and lowest possible costs. Depending on the used fuel the OC has to fulfill other requirements too. For hydrocarbon fuels a high catalytic activity is beneficial (especially for methane conversion). Ni-based carriers have a good catalytic activity and are suitable for methane combustion and reforming. Other possible metals besides Ni are: Cu, Fe, Co, Mn and Cd [1, 2, 10, 14, 24, 39, 55]. Most oxides have to be supported by other inert materials to gain the necessary mechanical strength and attrition stability to be operated in a CFB. Such support materials can be Al_2O_3 , TiO_2 or yttria-stabilized zirconia (YSZ) [35].

Four oxides, in favor of the ability to convert CH_4 to CO_2 and H_2O , were found out to be feasible for use as OC. These four are nickel, copper, iron and manganese. There are advantages and disadvantages for all oxides but especially nickel has thermodynamic restrictions. Fig. 14 shows the thermodynamic limitation of all four oxides. A part from the thermodynamic restrictions the oxygen transport capacity R_0 has a major impact of the suitability of an OC. Table 2 gives an overview of the oxygen transport capacity of the four metal oxides mentioned above.

Table 2 Oxygen transport capacity R_0 [kg/kg]

Redox system	Value
NiO-Ni	0.214
CuO-Cu	0.201
Mn_3O_4 -MnO	0.070
Fe_2O_3 - Fe_3O_4	0.033
Fe_3O_4 -FeO	0.067
Fe_2O_3 -FeO	0.101

The listed R_0 values represent values for pure metal oxides. As a specific particle consists of inert support material and active metal oxide, the particle oxygen transport capacity $R_{0,i}$ is smaller. Additionally, in the production process some of the active metal oxides are bounded in the inner structure of the particle. These metal oxides show in their activeness a dependency on the temperature. Therefore the actual oxygen transport capacity is depending on the composition of the particle, which is the $R_{0,i}$ of the particle, and the temperature. The more applicable parameter for particle characterization represents the value of $R_{0,i}$ as the actual oxygen transport capacity is hard to determine.

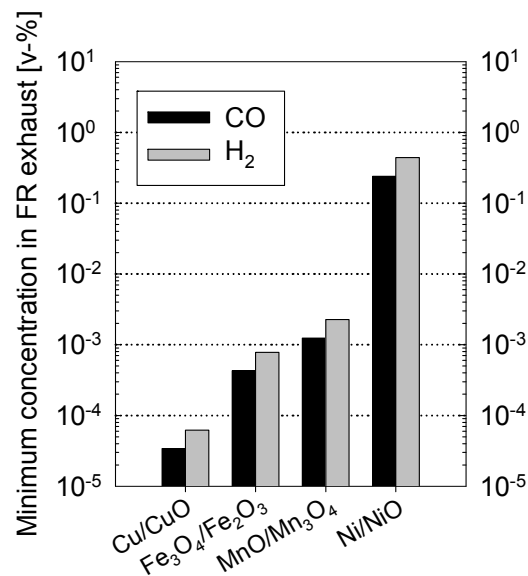


Fig. 14 Thermodynamic limitation of fuel conversion wet gas concentrations (fuel: CH₄; no steam added to the FR; Eqs. (3) and (4) in equilibrium; $T_{FR} = 850^{\circ}\text{C}$)

Another important factor is the active surface area available for solid gas reaction on the particle. The surface area is determined by the porosity of a particle and the particles reactivity, i.e. the amount of active metal oxide in the particle.

The melting temperature of most redox systems suits the operating conditions in a CL system. Only the melting temperature of Cu seems critical. ($T_{\text{melt, Cu}} \sim 1083^{\circ}\text{C}$, $T_{\text{melt, CuO}} \sim 1326^{\circ}\text{C}$)

Major contributions to the development work on oxygen carrier particles are done at Tokyo Institute of Technology, Chalmers University of Technology in Sweden, CSIC-ICB in Spain and Korean Institute of Energy Research. Up to 600 different materials were tested and screened up to now. More recently, CSIC and Chalmers contributed the majority in testing whereas all early developments were made at the Tokyo Institute of Technology [33].

2.4 REACTOR SYSTEMS FOR CHEMICAL LOOPING PROCESSES

In a chemical looping system there has to be an exchange of oxygen carrier between the oxidation and reduction zone. A circulating fluidized bed allows such a transport of particles. One reaction zone, e.g. the AR, can be designed as a riser reactor entraining solids and the second reaction zone, e.g. the FR, can be considered in the solids return leg of the first reactor. This zone can be either a bubbling bed or a second circulating fluidized bed. The loop of the oxygen carrier is closed via a connection between the second and first reaction zone. The use of loop seals, fluidized with inert gases, avoids mixing between the different gas streams in the reaction zones.

At Chalmers University of Technology a chemical looping combustion installation is successfully operated at a scale of 10 kW fuel power [36]. This installation works according to the concept shown in Fig. 15 with an AR as a circulating fluidized bed riser and the FR as a bubbling bed reactor in the return loop of the solids separated from the riser by moderately fluidized loop seals. From the principle's point of view, such a configuration is also successfully used for biomass gasification at a scale of 8 MW fuel power [16].

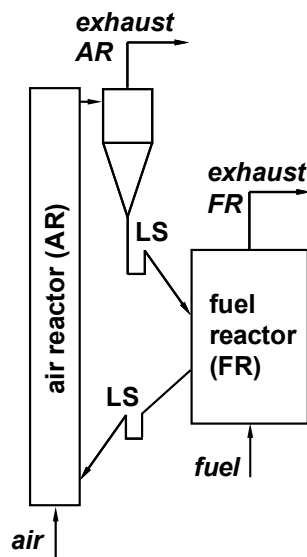


Fig. 15 The 10 kW chemical looping unit at Chalmers University of Technology [36], LS...loop seal)

Several CL prototypes have been presented in literature varying in size from 300 W at Chalmers University of Technology (based on bubbling fluidized beds) up to 145 kW at Vienna University of Technology (based on circulating fluidized beds). Different particles, from natural ore to synthetic particles, were used. The pilot rigs were operated with gaseous fuel as well as with solid fuel. More than 1000h of operation experience worldwide with different oxygen carrier are reported [33].

The classical application of dual zone fluidized bed concepts is the fluid catalytic cracking process (FCC), where carbon depositions on catalyst particles are burned off in a second reaction zone. Along with the progress in energy conversion technology, several technologies other than FCC but based on

the DFB approach have been proposed and have partly been successfully demonstrated. A brief overview is given in Table 3.

Table 3 Dual fluidized bed technologies apart from FCC [46]

technology	purpose of solids	importance of gas-solid contact
(biomass) gasification	heat transport, catalyst	partially for tar reforming in the gas generator
sorption enhanced reforming	CO ₂ and heat transport, catalyst	high in the reformer/carbonator, low in the re-calciner (heat-driven)
carbonate looping	CO ₂ (and heat) transport	high in the absorber/carbonator, low in the re-calciner (heat-driven)
chemical looping	oxygen and heat transport	high in both reactors, no gas phase conversion without solids

With respect to the necessary interaction of gases and solids in the system, especially chemical looping processes require high gas-solid interaction and sufficient contact time in both reactors.

Systems combining two CFB reactors have already been proposed for biomass steam gasification [40] and chemical looping processes [4, 5, 25]. The principal schemes of these concepts are sketched in Fig. 16. In both systems, the solids must pass at least two times a cyclone during one entire loop. The entrainment of both risers is crucially necessary in order to provide solids circulation between the two reactors. In the case of the system in Fig. 16b, partial back mixing of solids is possible on either side. For the 2-way loop seals measures need to be taken in order to control the flow rate of solids into each of the two loop seal outlets. In case the process requires high global circulation, such a back mixing loop means a higher solids load on the cyclones compared to the case without a solids flow back into the same reactor.

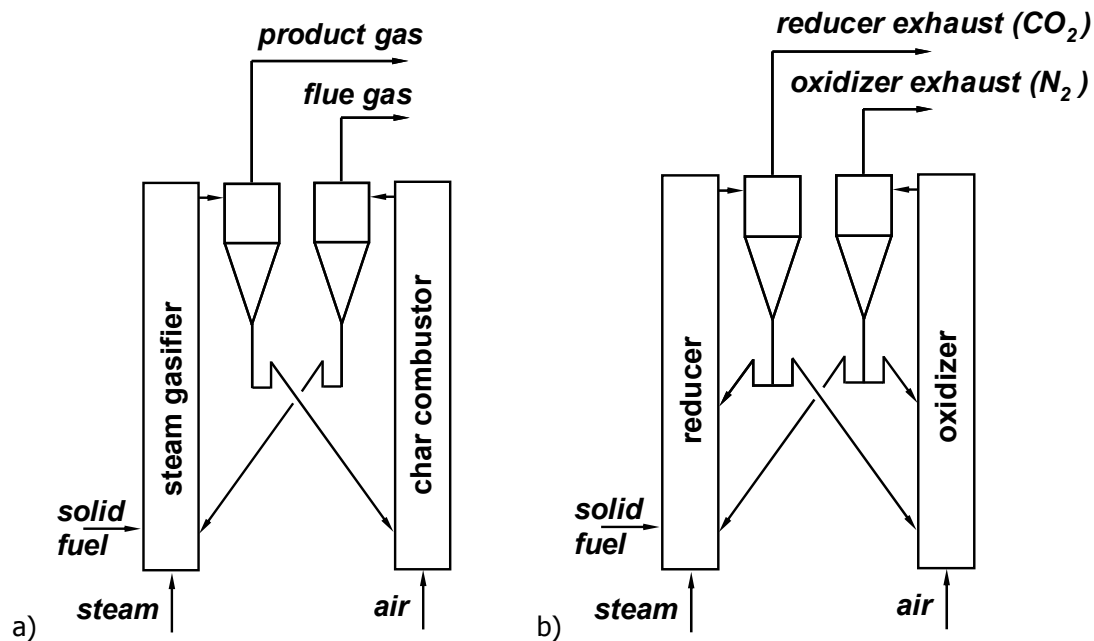


Fig. 16 Systems featuring two circulating fluidized bed reactors; a) Battelle/FERCO biomass gasifier [40], b) Alstom chemical looping reactor concept [4]

For CLC or CLR processes with selective oxygen transport by the bed material, the following basic requirements can be stated:

- High global solids circulation is beneficial in order to provide enough oxygen in the FR and in order to keep the temperature difference between AR and FR low.
- To obtain satisfactory gas conversion excellent gas-solids contact is required in both reactors. In CLC unconverted fuel in off gas of the FR will hardly be tolerable. An increase in gas-solid contact allows to decrease the needed solid inventory in both reactors
- Low particle attrition rates are appreciated especially if costly oxygen carriers are used.

Therefore, the system investigated in the present study represents a combination of the existing practice in CLC technology according to Fig. 15 with the idea to use two scale-up ready CFBs for both AR and FR. A second aim of the present effort is to propose a robust fluidized bed system which is most simple with respect to necessary bed material flow control devices.

2.4.1 DUAL CIRCULATING FLUIDIZED BED SYSTEM

In the dual circulating fluidized bed (DCFB) system according to Fig. 17, the two CFB reactors are interconnected via a fluidized loop seal in the bottom region of the reactors (lower loop seal). The entrainment of the left hand side reactor (AR) determines global solids circulation. The solids are separated from the AR exhaust stream in a cyclone separator and pass over through a fluidized loop seal (upper loop seal) into the right hand side reactor (FR). From there, the global solids loop closes via the lower loop seal. The FR features a circulation loop in itself (FR cyclone and internal loop seal) and may be optimized with respect to good gas-solid contact and low particle attrition rates. The

global circulation rate can be effectively controlled by staged fluidization of the AR. The direct hydraulic communication of the two CFB reactors allows stable solids distribution in the system as long as the lower loop seal is designed large enough to not significantly hinder solids flow. This reactor concept was demonstrated at a cold flow model [48] and at a 120 kW pilot rig for gaseous fuels [28] and was patented in the year 2008 [45].

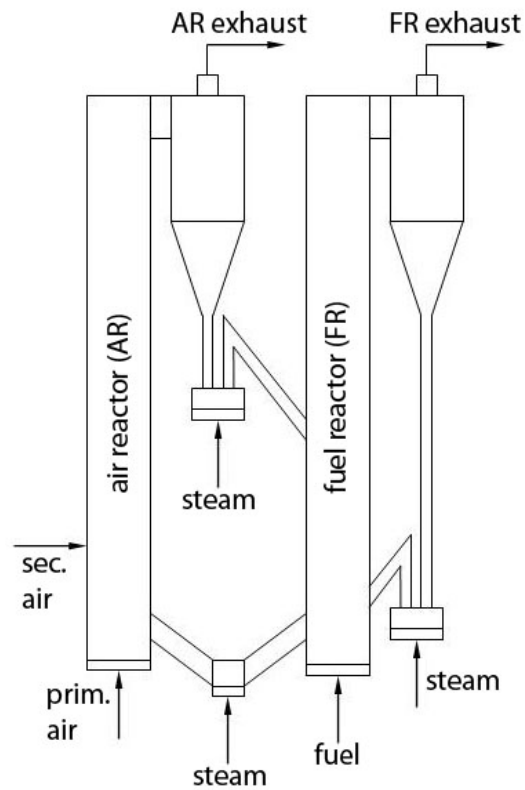


Fig. 17 Dual circulating fluidized bed reactor system

Apart from CLC, the DCFB system has some potential to be applied in other dual bed processes such as carbonate looping for end-of-pipe CO₂ capture [3], dual bed gasification and sorption enhanced reforming [13, 44].

3

EXPERIMENTAL

3.1 THE 120 KW DCFB PILOT RIG

The chemical looping pilot rig is a DCFB system, as described above, for gaseous fuels. This novel reactor system was especially designed for chemical looping process. In a first step a cold flow model was built to study fluid dynamics of the reactor system and verify the three basic requirements: good gas solid contact, high solid circulation and low solids loss.

The pilot rig is designed with a direct focus on scalability to larger size. In other words, the two reactors are stainless steel pipes with uniform cross section over the reactor height. The nominal operating parameters are:

- Global air/fuel ratio of 1.2 and
- Fuel load of 120 kW_{th} natural gas.

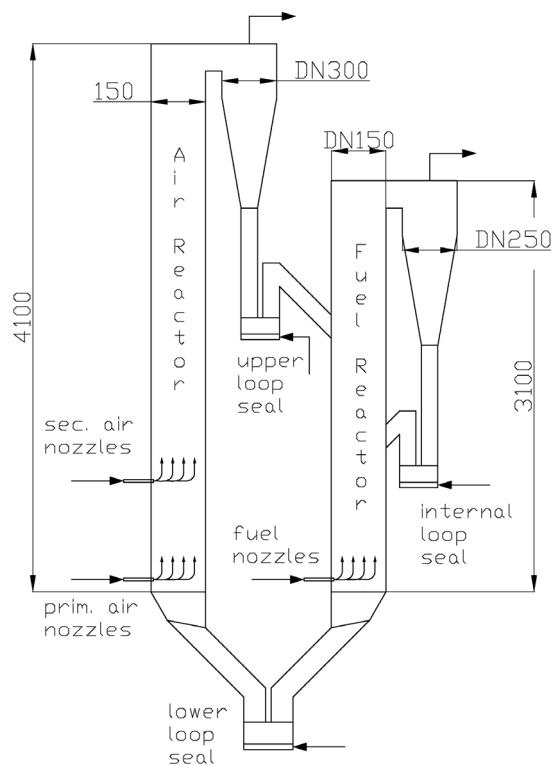


Fig. 18 Geometry of the 120 kW CLC pilot rig

To gain maximum flexibility in operation (CLC to CLR mode) compromises were made. These allow variation of global air/fuel ratio and fuel power without reconstruction. The hot commissioning phase was completed in early 2008.

The main geometry of the 120 kW CL pilot rig is shown in Fig. 18. The flow regime in the AR is fast fluidization and in the FR turbulent fluidization.

Loop seals between the reactors avoid mixing of AR and FR gases. These loop seals are fluidized with superheated steam and may be switched to air fluidization during start-up and shut-down. Downstream of each reactor, gas and solids are separated in cyclone separators. The cyclone separators are designed according to Hugi and Reh [18]. For means of simplicity at the small scale, the lower loop seal connecting the two reactors represents a continuation of the reactor bodies.

The main fluidization nozzles are arranged along the circumference of the cylindrical reactor shells. The pilot rig can be fueled with natural gas, C₃H₈, H₂, CO and mixtures of these gases. Additional trace gases can be added (e.g. H₂S) or inert gases (e.g. N₂) for partial pressure and reactor fluidization experiments.

In order to remove the heat from the reactor system and to control the temperature the AR shell is equipped with cooling jackets. This configuration allows independent control of one reactor temperature from the global air/fuel ratio. These cooling jackets are operated with gaseous cooling media (air or air/steam mixture). To operate the pilot rig at steady state a minimum heat release within the reactor system of approximately 60 kW is needed. For tests with less active OC (e.g. natural ores) support heat input in the AR is possible. This can be either done with air preheating or by introducing support fuel in the AR. An important parameter of fuel reforming is the steam/carbon ratio, which can be varied through addition of steam to the FR. In case of high bed material losses during operation, i.e. soft bed material which would lead to high attrition rates and high losses, bed material can be added discontinuously during operation. The properties of the pilot rig are summarized in Table 4. A detailed description of the reactor design, the cooling system and the other auxiliary units can be found in Kolbitsch et al. [28].

Table 4 Range of operating parameters of the CLC pilot rig

Parameter	Unit	value
fuel	-	natural gas, H ₂ , CO, C ₃ H ₈ , mixtures
fuel power	kW	60 – 155
global air/fuel ratio	-	0.4 – 1.5
bed material inventory	kg	55 – 90
Q _{loss}	kW	8 – 15 depending on operating conditions
Q _{cooling}	kW	0 – 70
air preheating	kW	up to 15
support fuel	kW	0 – 100
steam addition	kg/h	0 – 6

3.1.1 ARRANGEMENT IN THE LABORATORY

A process flow diagram of the whole pilot rig setup is shown in Fig. 19. The exhaust gas streams of the two reactors are cooled separately to about 300°C, depending on the operating conditions. An isokinetic particle sampling point and a gas sampling point at each exhaust gas stream are arranged after the cooling section. The cooled exhaust gas streams pass valves. These allow for imposing defined backpressure on each reactor. The exhaust gas streams are then mixed and post combusted in a fire tube boiler operated with natural gas. A third gas sampling point is arranged after the post combustion unit to determine the quality of the post combustion. For safety and environmental reasons the flue gas is filtered and then sent to the stack. The exhaust and flue gas cooling system is designed as an atmospheric pressure steam cycle. The steam is separated in the steam drum and can either be sent to the chimney or used for cooling the reactor system.

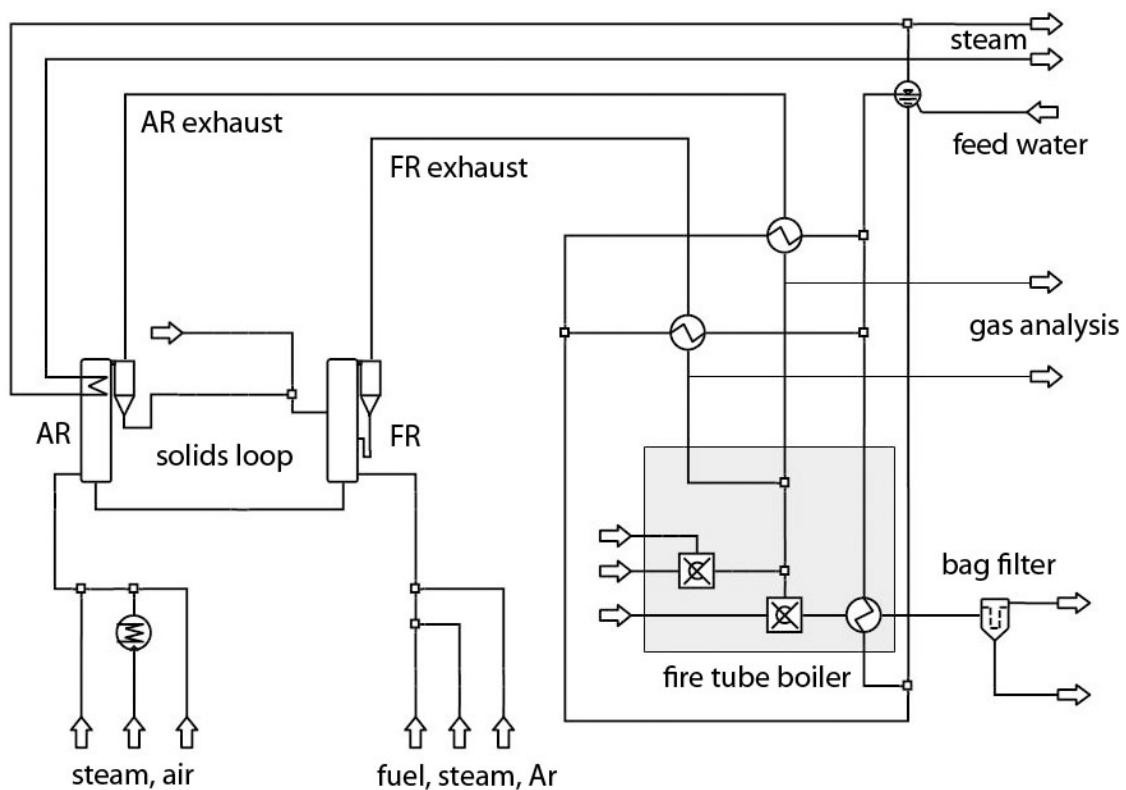


Fig. 19 Arrangement of CLC reactor and auxiliary units of the 120 kW CLC pilot rig

3.1.2 AUXILIARY EQUIPMENT

For safety and environmental reasons, a bed material handling device was designed and built. It consists of a bed material container with three conjunctions: one for the solid inlet, one for the solid outlet and one connected to a vacuum pump with an intermediate filter step. It allows handling of hazardous bed materials (e.g. Ni-based oxygen carriers) from bed material containers into the reactor and enables to refill bed material during operation. This way, the loss of fines to the surrounding lab and contact with the particles is minimized.

Another important piece of auxiliary equipment is the solid sampling device. It allows determination of the actual state of solid entering and leaving the FR. In the upper and lower loop seal solid sampling pipes are arranged. Particles are entrained through the pipe from the loop seals into the solid sampling device. The solid sampling device is cooled and filled with inert gas to prevent the solids from being oxidized. The inactive and cooled solid samples have to be further analyzed to determine the actual state of the sample. More details on the solid sampling device are reported by Kolbitsch et al. [29].

Another important auxiliary component of the pilot plant arrangement is the switch case. It supplies all electrical units with energy. It contains the programmable logic control which represents the interface between all electronic units (measurement converters, control valves, burners, filter, etc.) and data logging, visualization of the measurements and control unit. Together with all fuses, switches, sensors and alarm system it represents the backbone of the pilot rig.

3.1.3 GAUGE POINTS

The pilot rig is equipped with 31 pressure transducers, 35 thermocouples, 15 flow meters with local indication and three flow meters with online registration and local indication. The three gas sampling point of AR exhaust gas, FR exhaust gas and fire tube boiler flue gas are online analyzed.

The pressure transducer all measure pressure difference either between the gauge point pressure and the ambient pressure or between two pressure gauge points (e.g. bag filter pressure difference). The installed pressure transducers have a high zero point drift which makes a zero point adjustment necessary to increase accuracy of measurement.

The flow meters with online registration measure the main inlet flows into the reactor, i.e. the fuel flow into the FR and the air flow into the AR. The other flow meters measure flows of the startup burner, of the post combustor, of the loop seal fluidization, of the synthetic gas mixing station and of the support fuel input to the AR.

The raw gas of the gas sampling points has to be prepared for gas analysis. First a heated dust filter removes any fines, second the gas sample is transported via a heated Teflon tube to a sample gas cooler which condenses water continuously down to a dewpoint of 5°C out of the gas sample. The dried gas is then transported to the gas analyzer station. All three gas sampling streams are prepared in that way. Periodic maintenance work has to be done especially on the dust filter and on the Teflon tubes to guarantee reliable and reproducible measurements. It is indispensable to calibrate the gas analyzers for accurate gas concentration measurement with special attention to the gas chromatograph.

3.2 EXPERIMENTAL CAMPAIGN

3.2.1 EXPERIMENT PREPARATION

The nominal solid inventory for particles with high attrition resistance is approximately 65 kg. Prior to each experiment the solids inventory is reduced to approximately 55 kg for start-up. At higher solid inventory, the bed material interferes with the start-up burner which leads to continuous malfunction. A further decrease in inventory would lead to a reduced global solids circulation which makes it impossible to reach the desired operation temperature in an acceptable start-up time.

It turned out to be beneficial to turn on all electronic devices a day before the experiment to guaranty steady state operating temperature of any electronic converters. This reduces the measurement drift of the converters.

As described above the calibration of the gas analyzers is essential. The quality of the data determines the performance of the pilot rig for a certain experiment. Therefore, in the erection phase of the pilot plant, special focus was drawn on the sample gas preparation and the gas analysis setup.

3.2.2 START UP PROCEDURE

The first step for start-up is ventilation of the whole pilot rig with cold air. Therefore, air is introduced in both reactors: starting with the FR, the lower loop seal, the internal loop seal the AR and finally the upper loop seal. Additional air is introduced at the startup burner and the fire tube burner. After ventilation the fire tube burner is ignited this assures full combustion of all gases before entering the stack. The startup burner is then ignited and the air-preheater for the AR is turned on. Special attention has to be drawn to the startup burner flue gas temperature (not to exceed 1050°C) and the nozzle velocity of the AR (not to exceed 50 m/s). At approximately 500°C, H₂ is introduced in the FR which reacts with the available O₂ from the lower loop seal in the dense bed region of the FR. At this time a very steep temperature increase is observed. As soon as the AR reaches 500°C, H₂ is also introduced in the AR. This way the pilot rig is heated up to approximately 700°C. At this temperature, H₂ is substituted with C₃H₈ to increase energy input at same volume flow. As soon as operating temperature of approximately 900°C is reached the remaining bed material for the experiment is introduced. Therefore, the startup burner is turned off, the fluidization in both reactors is turned down to minimum and with the aid of the bed material handling device the desired amount is pneumatically transported in the reactor. A check list helps the plant operator to accomplish the startup procedure.

The loop seal fluidization agent is changed to steam once all of the necessary bed material is filled into the reactor, operating temperature is reached and the startup burner is turned off. Special attention is required switching from air to steam as the fluidization in the loop seal stops for some seconds. Finally, the FR is fluidized with the desired fuel. With this step, the CLC operation starts and the start-up procedure is finished.

3.2.3 CHEMICAL LOOPING OPERATION

For steady state operation different controllers have been installed. Operating power is controlled via a fuel control valve. In cases of alternative fuels from gas cylinders (i.e. H_2/CO , C_3H_8), the fuel flows have to be controlled manually. For the regulation of the global air/fuel ratio, the main air inlet is also equipped with a control valve. An additional control valve determines the degree of air staging between primary and secondary air.

To keep the operating temperature constant the cooling power can be adjusted manually. Air and air steam mixture introduced in two separate cooling jackets at the AR allow regulation of the cooling power up to 70 kW. The third cooling jacket, designed as evaporator, could be reconstructed for gaseous cooling media for increased cooling power. A more detailed description of the cooling system can be found in the PhD thesis of Philipp Kolbitsch [26].

3.2.4 SHUT DOWN PROCEDURE

For shut down, the fuel is substituted with N_2 to remove all combustible gases in the FR. This can be checked by the gas analysis of the FR before the FR fluidization agent is changed to air. All volume flows in the reactor system are changed to nominal values for shut down. Finally, the fire tube burner is shut down and the loop seal fluidization agent is changed back to air. With this operation, the system is cooled down to approximately 300°C. At this temperature, AR, FR and loop seal fluidization is turned down to minimum. After another 12h, the solids in the reactors are cooled down to ambient temperature and the fluidization is turned off.

3.2.5 ONLINE DATA ACQUISITION SYSTEM

The obtained data from all electronic measurements are averaged and recorded in defined intervals. Additionally, in real time operation important operating parameters such as fuel power, global air/fuel ratio and gas conversions are calculated from the raw data. These parameters are used for proper operation of the pilot rig.

3.2.6 SOLIDS SAMPLING

Solids sampling in the upper and the lower loop seal during operation delivers important information about the state of the CL system. With the aid of the solids sampling device, as described above, particles can be entrained and preserved in their actual state (e.g. degree of oxidation). Special attention should be turned to the necessity to withdraw a sample big enough for evaluation. In general, the sampling procedure has to be done with great cautiousness.

3.2.7 EXPERIMENTAL EVALUATION

Solid sample evaluation

In CL systems, the determination of solids state allows the calculation of solids circulation rate for a certain operation point. Therefore, the samples are scaled to determine the mass m_0 and placed in a furnace for oxidation. The samples are then heated up to 1000°C and kept at this temperature for three hours. After cooling down to ambient temperature the sample is scaled again. Then the mass of the fully oxidized sample m_{ox} is determined. From these values, the mass fraction Ω_i of the sample can be calculated.

$$\Omega_i = \frac{m_{0,i}}{m_{ox}} \quad i = AR, FR \quad (13)$$

The mass fraction difference $\Delta\Omega$ between AR and FR (14) defines the mass flow of circulating solids. Equation (15) describes the relationship of combustion efficiency η_{comb} , oxygen demand of the fuel O_{min} , fuel flow \dot{m}_{fuel} and solid circulation $\dot{m}_{OC,ox}$.

$$\Delta\Omega = \Omega_{AR} - \Omega_{FR} \quad (14)$$

$$\dot{m}_{OC,ox} = \eta_{comb} \frac{O_{min} \dot{m}_{fuel}}{\Delta\Omega} \quad (15)$$

If the fully reduced state of the OC m_{red} is specified a more comprehensive value, the solids conversion $X_{S,i}$ of the OC, can be derived from the solid sampling evaluation. $X_{S,i}$ is defined by

$$X_{S,i} = \frac{m_{0,i} - m_{red}}{m_{ox} - m_{red}} \quad i = AR, FR \quad (16)$$

More details on the solid sampling procedure and an error assessment are reported by Kolbitsch et al. [29].

Mass balance of the bed inventory

The mass balance of the bed inventory in the reactor system is closed by documentation of all input and output quantities. The time and effort for emptying the reactor system is great and the probability of contamination of the surrounding laboratory environment with hazardous bed material should be minimized. Therefore, the total amount of solids samples as well as the amount of fines in the filter is documented. It is important to clean the filter bags before scaling the filter container.

Data evaluation with IPSEpro

The raw data are recorded as mean values of defined intervals. These values are evaluated by means of mass and energy balancing. Additionally, redundant measurements are reconciled and parameters are derived which cannot be measured directly (e.g. circulation rate, heat loss, wet gas concentration, etc.). A more detailed description can be found in the chapter on process modeling and simulation.

3.3 HEALTH SAFETY AND ENVIRONMENT ANALYSIS

Because of the involved substances and the prevailing high temperatures, measures must be taken to reduce the risk for health and safety of the operating staff to a minimum. A HAZOP study has been carried out to assess the events that may possibly lead to malfunction or hazardous situations during plant operation. The most serious hazards that must be avoided are:

- inflammable or explosive gas atmosphere in a part of the system
- leakage of inflammable or toxic gases to the laboratory environment
- leakage of bed material to the laboratory environment

Practically, all the assessed cases where a dangerous situation cannot easily be corrected by the control system or by manual correction of wrongly adjusted hand valves, a well-defined emergency shut-down procedure (ESDP) is to be followed. The ESDP mainly consists of an immediate interruption of natural gas supply what will cause the reactions to stop and make the system cool down. The natural gas supply pipes including the gas compressor are in the same time flushed with nitrogen in order to remove combustible gas completely from the system.

4

PROCESS MODELING AND SIMULATION

4.1 THE SIMULATION SOFTWARE IPSEPRO

IPSEpro is a stationary, equation orientated simulation software. It has a modular structure consisting of the user interface (process simulation environment, PSE), the model library and the equation solver (Kernel). The program structure allows fast solving time of some seconds and the model development kit is beneficial for the user as the user is enabled to edit the source code of the standard models as well as to create new models for special tasks. A more detailed description on the IPSEpro simulation software can be found elsewhere [41].

Due to the relative novelty of the CL-based processes, solid properties and gas-solid reactions were implemented in a new model library called advanced energy technology library (AET-Lib), which is an extended version of a comprehensive model library previously built for gasification-based processes [43]. The created CL model was validated by measurements of the 120 kW pilot rig.

4.2 CHEMICAL LOOPING SIMULATION MODEL

4.2.1 SUBSTANCE CLASSES AND THERMODYNAMIC PROPERTIES

In order to describe the composition and thermodynamic state of the streams involved in the process, different classes of substances are distinguished in the AET-Lib:

- pure water/steam
- mixtures of ideal gases
- organic substances (solid or liquid fuels)
- inorganic solids (active and non-active bed material components, ash components, etc.)

The organic substances in the AET-Lib consist of the six elements C, H, O, N, S, and Cl. These elements also represent – together with the air component Ar – the basis for all gaseous compounds modeled. The 40 inorganic solid substances modeled further contain the elements Na, K, Mg, Ca, Ti, Zr, Mn, Fe, Co, Ni, Cu, Zn, Al, and Si. Apart from the water/steam stream, which consists of a pure substance, the substance streams consist of mixtures of pure substances defined by the mass or molar fractions of the different species. The information contained in the stream composition further allows the calculation of mean molar mass, the mean standard enthalpy of formation, and methods for the calculation of temperature and pressure dependent properties of the mixture (enthalpy, entropy and density). The IAPWS-IF97 formulation [60] is used for calculation of the properties of

water and steam, the ideal gas data is formulated according to Burcat and McBride [9] and the inorganic solids data are calculated from polynomials fitting the data tables reported by Barin [6].

4.2.2 THERMODYNAMIC EQUILIBRIUM FORMULATION

Knowledge of the thermodynamic properties allows the calculation of thermodynamic equilibrium constants via minimization of Gibbs free enthalpy:

$$\ln K_p(T) = \frac{-\Delta G_R^0(T)}{R \cdot T} \quad (17)$$

The actual state of a substance combination with respect to the equilibrium of a specific chemical reaction

$$\sum_i \nu_i \cdot A_i = 0 \quad (18)$$

is expressed by the logarithmic deviation from equilibrium:

$$p\delta_{eq} = {}^{10}\log \left(\frac{\prod_i (p_i)^{\nu_i}}{\prod_i (p_i^*)^{\nu_i}} \right) = {}^{10}\log \left(\frac{\prod_i (p_i)^{\nu_i}}{K_p(T)} \right) \quad (19)$$

Definition of $p\delta_{eq}$ allows comfortable handling of equilibrium calculations in the simulation. For a prescribed gas composition at defined temperature and pressure, the value of $p\delta_{eq}$ can be calculated from equation (19). If $p\delta_{eq}$ is prescribed to be zero, the system is forced to adjust the gas composition (or, theoretically the temperature) in order to fulfill the thermodynamic equilibrium of the specific reaction. Values of $p\delta_{eq}$ below zero mean that the actual gas composition is on the left hand side of the reaction equation (where $\nu_i < 0$) and values above zero indicate that the actual gas composition is on the right hand side of the reaction equation (where $\nu_i > 0$). This simple approach allows plausibility checks for measured data with respect to the second law of thermodynamics and can be a robust method to predict a gas composition after validation with measured data, i.e. if it turns out that a certain reaction typically reaches equilibrium for certain operating conditions.

4.2.3 REDOX SYSTEMS AND REACTIONS MODELED

The redox systems implemented in the AET-Lib are presented in Table 5. In each gas-solid reactor unit, one active redox system must be specified. The global reaction of fuel oxidation (see Chapter 2.1 equ. (1)) must be divided into elementary steps for an adequate description of the FR. The hydrocarbon conversion is modeled by definition of conversion rates X for CH_4 , C_2H_4 , C_2H_6 , and C_3H_8 . Because the typical operating conditions of CLC systems would lead to practically complete conversion of hydrocarbons in equilibrium, no equilibrium formulations are made involving these species. For description of the oxidation of CO and H_2 the following reactions have been chosen:



Only in the case that no carbon fuel is introduced in the FR (i.e. oxidation of H₂ or reduction of H₂O), the direct oxidation of H₂ with the oxygen carrier is formulated instead of reactions (20) and (21):



In the case of the redox system CaSO₄/CaS, the H₂S formation reaction is additionally formulated in the FR model:



In the AR, the re-oxidation reaction (2) of the oxygen carrier is directly formulated.

It is important to notice that thermodynamic equilibrium of the redox-reaction can only be prescribed in either FR or AR depending on where the gas phase provides an excess of reactive species. In other words, if the O₂ supply to the AR is larger than needed for complete conversion of the fuel, thermodynamic equilibrium of reactions (20) and (21) may be reached in the FR while the excess O₂ will leave in the AR exhaust and reaction (2) cannot be in equilibrium in this case. If, on the other hand, oxygen is limited in the system, the AR side may react towards equilibrium of reaction (2) while in the FR exhaust only the CO-shift reaction (20) may react towards equilibrium while reaction (21) cannot be forced to be in equilibrium in this case. Apart from these formal restrictions, the decision whether a reaction can be assumed to be in equilibrium for a predictive simulation must be supported by experimental data for the respective fuel, oxygen carrier and reactor system.

Table 5 Redox systems implemented in the model library

Cu	Fe	Mn	Ni	Co	CaS
Cu/CuO*	Fe/FeO	Mn/MnO	Ni/NiO*	Co/CoO*	CaS/CaSO ₄ *
Cu/Cu ₂ O	FeO/Fe ₃ O ₄	MnO/Mn ₃ O ₄ *	*) redox system important for CL		
Cu ₂ O/CuO	Fe ₃ O ₄ /Fe ₂ O ₃ *	Mn ₃ O ₄ /Mn ₂ O ₃	Support materials implemented: Al ₂ O ₃ , CaAl ₂ O ₄ , MgAl ₂ O ₄ , CuAl ₂ O ₄ , NiAl ₂ O ₄ , SiO ₂ , TiO ₂ , ZrO ₂		
		Mn ₂ O ₃ /MnO ₂			

It turns out that black box models which fulfill the energy balance, the mass balances with respect to the chemical elements, and include information on possible reaction paths as well as equilibrium formulations in the way described above already allow a comprehensive description of CL reactor systems. On this basis, the specific problem definition for more detailed reactor models based on hydrodynamics and chemical kinetics is possible. It should be kept in mind that every step towards a

more detailed description of the phenomena should be justified by the availability of adequate measured data for model validation.

4.2.4 SIMULATION FLOW SHEET OF THE CLC PROCESS

The typical reactor system for CL is a circulating fluidized bed (CFB) with the riser as the AR and the FR in the return loop of the solids [35], as described in Chapter 2. Fig. 20 shows the representation of a basic CL configuration in the modeling environment. The loop seal fluidization, which is typically done with steam, is not separately shown in Fig. 20. The respective amounts of steam can be added to the gas streams into the reactors for the calculation. The solids are circulated between the two reactors, where they change in composition and temperature. The amount of new oxygen carrier continuously added can be theoretically zero if no bed material is lost as dust load on the gas streams. For means of completeness, a continuous removal of oxygen carrier is modeled.

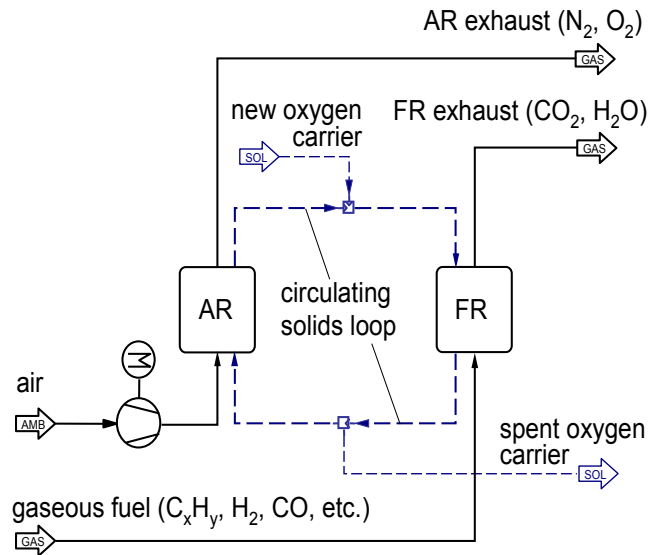


Fig. 20 Basic process configuration of a CLC system

4.2.5 RECONCILIATION OF DATA DERIVED PARAMETERS

The simulation software IPSEpro is applied for measurement validation by mass- and energy balance checking. The simulation result represents a steady state operating point of a plant. For an over-determined system another solver can be used, the method of Lagrange multipliers. A least squares problem for the deviation between measured value and equilibrated solution has to be solved.

$$\sum_i \left(\frac{x_i - \bar{x}_i}{tol_{x_i}} \right)^2 \rightarrow Min \quad (24)$$

The absolute tolerances tol_x account for varying units and include information about the quality of the measured value. Comparison between calculated errors and estimated tolerances allows the localization of systematic errors in both simulation and measurements. After exclusion of systematic

errors and adjustment of tolerances to reasonable values, the simulation describes the actual plant operation best within the limits of the model structure. Besides the validation of the measured quantities, all process variables that are not directly measured are known then from simulation. This is essential for quantities, which practically cannot be easily measured (solid circulation rate, heat extraction, solid composition, gas composition, etc.).

Fig. 21 shows the simulation model of the laboratory arrangement as it is used for data validation. The solids are circulated between the two reactors, where they change in composition and temperature. The amount of new oxygen carrier continuously added can be theoretically zero if no bed material is lost as dust load on the gas streams.

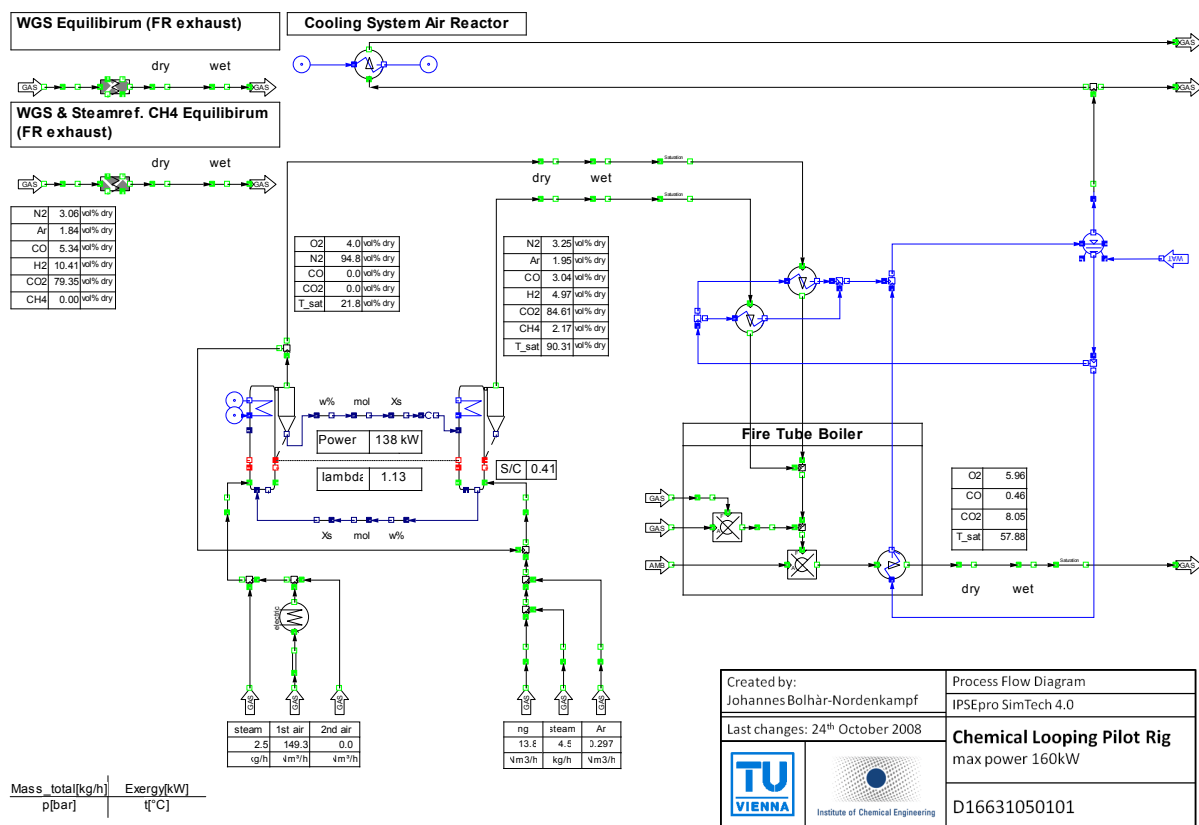


Fig. 21 Simulation model of the pilot plant fuelled with CH₄ at a global air/fuel ratio 1.13

There are 52 measurements (temperature, pressure, volume flows, oxidation state of the oxygen carrier, gas concentration of the exhaust gases, etc.) imported into the flow sheet. Those values, the flow sheet and the equations from each unit build an over-determined system which has a redundancy of 10. The tolerance tol_x of each measurement is on one hand influenced by the measurement error of each device or the standard deviation of the measured value, respectively. On the other hand it is influenced by the installation of each device, especially for thermocouples. All this has a major influence on the accuracy of the measurement. The experience from other pilot rigs helped to determine the tolerance for each device. The reconciled solution describes, within the limits of the model structure, the investigated steady state best. Besides the validation of the measured

quantities, two important process variables, the solid circulation rate and the heat extraction that are not directly measured are known then from simulation. Other process parameters, gas composition, solid composition and dilution of the FR exhaust gas by gas leakages from the AR, are also determined by the simulation.

In the following table an example of measurement values (bold) for the gas concentration in the FR exhaust gas and the AR exhaust gas versus reconciled values is shown.

Table 6 Example of reconciled solution for CLC operation at 142 kW CH₄ $\lambda=1.1$ T_{FR}=901°C)

AR exhaust gas concentration [vol-% _{dry}]			FR exhaust gas concentration [vol-% _{dry}]		
species	raw values	reconciled values	species	raw values	reconciled values
O₂	3.67	3.58	CO₂	75.03	74.71
CO₂	0.08	0.00	H₂	11.01	11.08
CO	0.00	0.00	CO	7.25	7.25
N ₂	95.46	95.28	N₂	3.59	3.50
Ar	1.14	1.14	Ar	1.33	1.70
			CH₄	1.31	1.76
sum	100.35	100.00		99.69	100.00

From the gas compositions in the AR and FR exhaust gas, leakage and dilution can be determined. It is most likely that there is no leakage from FR to AR as there is no CO₂ in the AR exhaust gas. The CO₂ value shows a small deviation from zero which lies within the error of the used instrument. The N₂ content in the fuel (see Table 7) cannot explain the measured N₂ concentration in the FR exhaust gas. Therefore, some dilution from AR to FR takes place, most likely through the upper loop seal.

Table 7 Natural gas composition

species	conc.[vol-% _{dry}]
CH ₄	97.374
C ₂ H ₆	0.994
C ₃ H ₈	0.268
higher C _x H _y	0.168
CO ₂	0.265
N ₂	0.931

Apart from the validation of the measured values, three important process variables, i.e. the solids circulation rate, the extracted heat and the dilution from AR to FR, are determined with the simulation model. Fig. 22 shows the extracted heat of the pilot plant at constant fuel load and constant FR temperature. The dashed line represents the extracted heat at maximum conversion to equilibrium. Naturally, the maximum heat release is at a global air/fuel ratio of 1. The solid line represents the

extracted heat from measured data. At global air/fuel ratios ≤ 0.9 maximum fuel conversion is reached and the chemical reactions reach equilibrium. At global air/fuel ratios > 0.9 a deviation from the calculated heat extraction for maximum conversion to equilibrium is observed. A decrease in CH_4 conversion and deviations from equilibrium explain this trend.

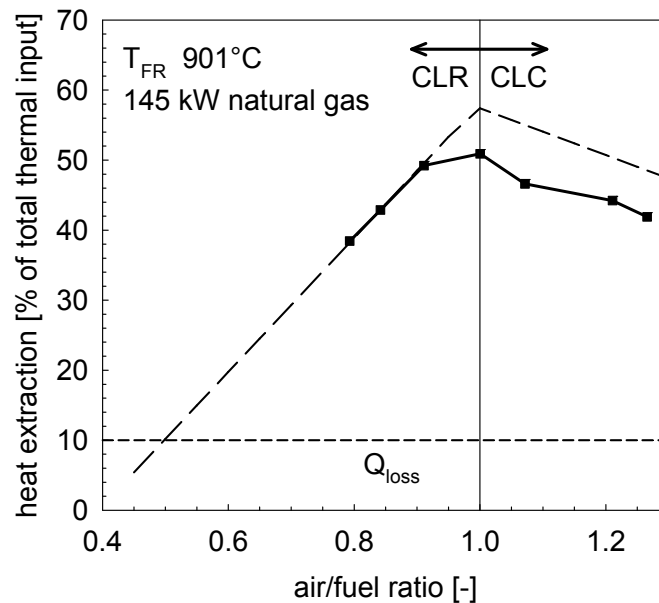


Fig. 22 Extracted heat versus global air/fuel ratio for typical operation conditions

The determination of the heat loss Q_{loss} of the reactor system allows an approximation of the theoretical minimum global air/fuel ratio at which the reactor system can be operated.

The simulation of complex power plant cycles based on the basic CL configuration in Fig. 20 is possible since the IPSEpro environment is especially dedicated to power plant optimization. Details can be found in chapter 6.

It should be mentioned that the model library has been already used in the design phase of a 120 kW fuel power test facility including a steam generation system and several downstream elements like post-combustor and bag filter [28].

5

RESULTS FROM 120 kW PILOT PLANT

5.1 CLC EXPERIMENTAL RESULTS

In CLC-StR, as described in Chapter 2.2.2, the CL unit utilizes a steam reformer with heat. Therefore the reactor system is operated in CLC mode. The presented results summarize the CLC experiments described in detail in the thesis of Philipp Kolbitsch [26].

Three different oxygen carriers were investigated. For hot commissioning and first operating experience a natural ore, ilmenite, was used. Additionally, two different batches of the desired Ni-based particles were tested. A summary of the OC characterization is listed in Table 8.

Table 8 OC characterization: ilmenite, OC-A (NOV1sd), OC-B (S1)

parameter	unit	ilmenite	OC-A (NOV1sd)	OC-B (S1)
active material		Fe ₂ O ₃ /FeO	Ni/NiO	Ni/NiO
inert material		manly TiO ₂ , MgO, SiO ₂	NiAl ₂ O ₄	NiAl ₂ O ₄ , MgAl ₂ O ₄
active material content	wt%	~48	~40	~40
R _{0,i}	kg/kg	0.04849	0.08568	0.08844
d _p	µm	100 – 400	90 – 212	90 – 212
based on data from		Titania A/S	Jerndal et al. [23]	Linderholm et al. [32]

The first results represent experiments with the nonhazardous natural ore ilmenite. The pilot rig is fueled with three different gases, CO, H₂+N₂ and CH₄. The fuel power input for all gases is approximately 80 kW. The highest conversion is seen with H₂ of approximately 92%. The CO conversion is significant lower at approximately 62%. An even further decrease is observed with CH₄ as fuel. The conversion drops to 40%. Varying the fuel load to lower values the fuel conversion of CO and CH₄ increases due to higher OC/fuel ratio. It is important to notice that those values represent preliminary results and there is still room for improvement.

After those first experiments the Ni-based particle OC-A is tested. Again three gases, CO, H₂+N₂ and CH₄, are used as fuel. The conversion of H₂ in CLC mode is very close to the thermodynamic maximum, whereas the CO conversion is somewhat lower. Those experiments show a very high reactivity of the OC-A compared to ilmenite. In a second series of experiments CH₄ at a fuel load of 140 kW is used. In CLC mode the maximum CH₄ conversion of 0.95 and CO₂ yield of 0.89 is reached at a FR temperature of 950°C and a solid inventory of 65 kg. In Fig. 23 a temperature variation at a global air/fuel ratio of approximately 1.1 is shown. CH₄ conversion and CO₂ yield is promoted with increasing temperature but the CH₄ conversion reaches a maximum at 900°C. The decrease in

conversion is probably due to a change in the Ni/NiO ratio in the particle with increasing temperatures. More information on the performance of the OC-A with H₂, CO and CH₄ and the influence of the solids conversion on the performance can be found at Kolbitsch et al. [27, 30].

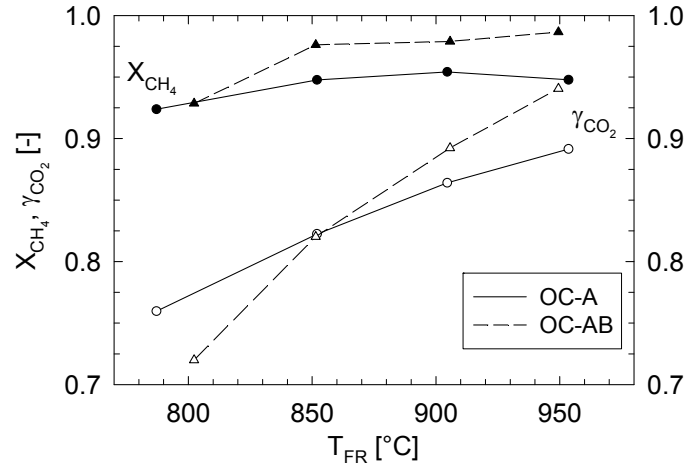


Fig. 23 CH₄ conversion X_{CH_4} and CO₂ yield γ_{CO_2} vs. FR temperature (global air/fuel ratio ~ 1.1)

The second Ni-based OC is only test with CH₄ as fuel. The produced amount of the OC-B is insufficient to operate the pilot rig with it only. Therefore, OC-B is mixed with OC-A in a ratio of 1:1 and henceforth termed OC-AB. The comparison, shown in Fig. 23, between OC-A and OC-AB shows a higher performance of the mixture of particles for almost all temperatures. The CH₄ conversion shows only small FR temperature dependency where as the CO₂ yield has a steep decay with decreasing FR temperature. The change in performance can be explained by a decrease in oxygen transport within the OC and thus increases the Ni content on the OC surface as reported by Jerndal et al. [23]. In other words, the metallic Ni on the surface catalytically supports the steam reforming reaction of CH₄ which leads to a faster decay of CH₄. As the reactor height of the pilot rig is limited (only 3 m) due to the surrounding laboratory a further improvement in performance at industrial scale seems feasible by increasing the gas residence time. Table 9 gives a summary of the maximum conversions achieved with the three OCs.

Table 9 Maximum H₂, CO, CH₄ conversion and CO₂ yield (ilmenite, OC-A, OC-AB)

parameter	ilmenite	OC-A	OC-AB
H ₂ conversion	0.92	0.99	-
CO conversion	0.62	0.98	-
CH ₄ conversion	0.42	0.95	0.99
CO ₂ yield	0.38	0.89	0.92

5.2 CLR EXPERIMENTAL CAMPAIGN

A 120 kW chemical looping pilot rig has been designed and operated, as described in Chapter 3.1. The presented results focus on the FR reforming performance at three different temperatures and on an analysis of the AR oxygen absorption performance.

The pilot rig has been operated from 750°C to 950°C in the FR and from a global air/fuel ratio of 1.5 down to autothermal CLR operation at global air/fuel ratios between 0.45 and 0.52. For all experiments presented in this chapter the CL unit is fueled with natural gas at a rate that corresponds to approximately 140 kW fuel power.

The natural gas from Vienna's gas grid consists mainly of methane (more than 97 vol-%_{dry} CH₄). The detailed fuel composition can be found in Table 7.

A highly active OC manufactured by the Flemish Institute for Technological Research (VITO), Belgium under the guidance of Chalmers University of Technology, Sweden is used. The OC is based on NiO, α -Al₂O₃ and MgO. After sintering the particles consist of active NiO and inert NiAl₂O₃ and MgAl₂O₃. More information on the OCs used can be found by Jerndal et al. [23]. The mean particle size of the OC is approximately 120 μ m.

The presented results show graphs for the four gas species H₂, CO, CO₂ and CH₄ versus the global air/fuel ratio. During variation of the global air/fuel ratio the fuel power, FR temperature and the steam to carbon ratio are kept constant with only small fluctuations. Additionally, the FR is operated at three temperatures, approximately 900°C, 800°C and 750°C. In all diagrams the solid lines represent the values as measured at the pilot unit whereas the dashed lines represent the thermodynamic equilibrium calculated by minimization of Gibbs free enthalpy (JANAF data, formal reactions (7) and (8)). All measured values represent reconciled solutions that fulfill mass and energy balances.

Fig. 24 shows the synthesis gas composition at a FR temperature of approximately 903°C. One can observe a decreasing CH₄ concentration with decreasing global air/fuel ratio. The thermodynamic equilibrium concentration of CH₄ is close to zero at 1 bar(a) and 900°C for all global air/fuel ratios. The graphs of the other gas species run along the equilibrium concentrations with small deviations mainly due to incomplete CH₄ conversion at global air/fuel ratios > 0.8. The global air/fuel ratio is varied down to approximately 0.52, where operation is autothermal, i.e. no reactor cooling is required. This ratio is determined by the heat loss of the pilot rig and by the heat withdrawn with the hot gas streams. All these quantities depend on the operating temperature. At an global air/fuel ratio of 0.5 and an S/C ratio of approximately 0.4 (considering all loop seal steam from the lower loop seal to enter the FR, what is a worst case scenario and it is likely that the actual S/C ratio in the FR is much lower than 0.4), the H₂/CO ratio in the synthesis gas reaches a value of 2.0.

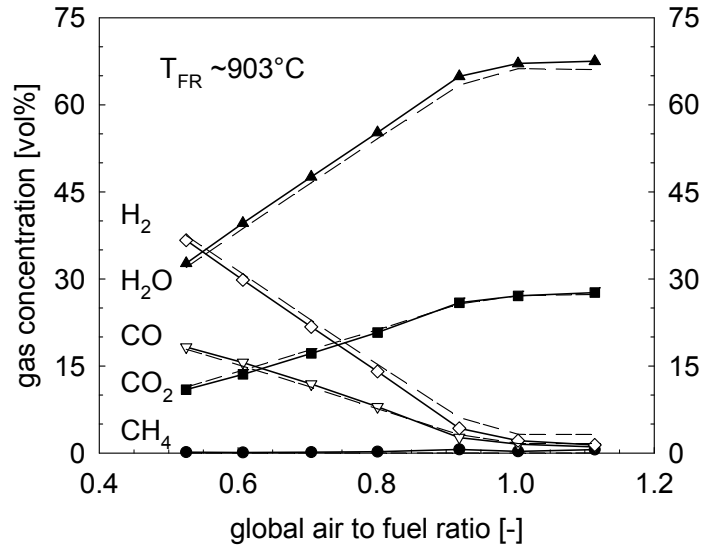


Fig. 24 Wet-gas concentration in the FR exhaust gas at 903°C 140 kW natural gas and S/C =0.4

To maximize the ratio of H₂/CO the temperature can be reduced. The energy balance of the reactor system has at any time to be fulfilled which determines some limiting constraints, such as global air/fuel ratio, reaction velocity and coke formation. Fig. 25 and Fig. 26 show the gas species H₂, CO, CO₂, CH₄ in the FR exhaust gas (i.e. in the raw synthesis gas) at two lower temperatures of 798°C and 747°C, respectively. Again, methane conversion is incomplete at higher values of the global air/fuel ratio. The other graphs run along the equilibrium lines. In some operating points the thermodynamic equilibrium is reached. At the lowest global air/fuel ratio of 0.5 at a temperature of 798°C and a steam/carbon ratio of approximately 0.4, the ratio of H₂/CO is increased to 2.4. A further increase in the H₂/CO ratio can be seen by lowering the temperature further to approximately 747°C. At a global air/fuel ratio of 0.51 and a steam/carbon ratio of 0.4 another 10% increase to 2.6 can be observed. A further decrease of the global air/fuel ratio down to 0.46 at a FR temperature of 747°C a small increase in of the H₂/CO ratio can be seen.

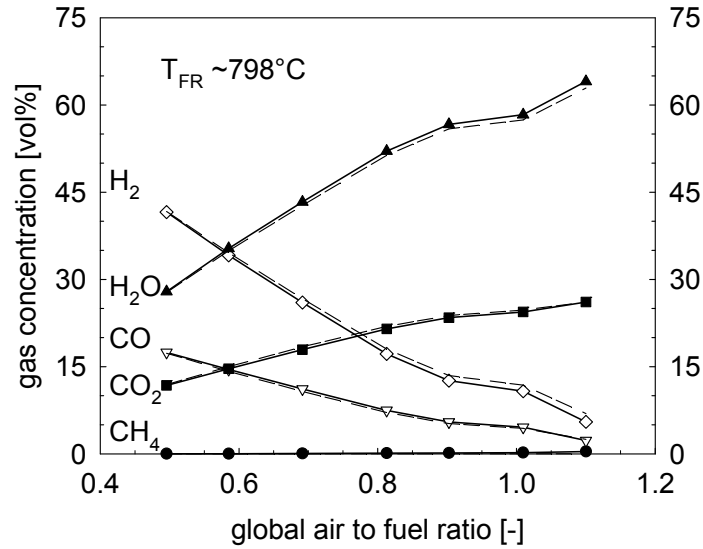


Fig. 25 Wet-gas concentration in the FR exhaust gas at 798°C 140 kW natural gas and S/C =0.4

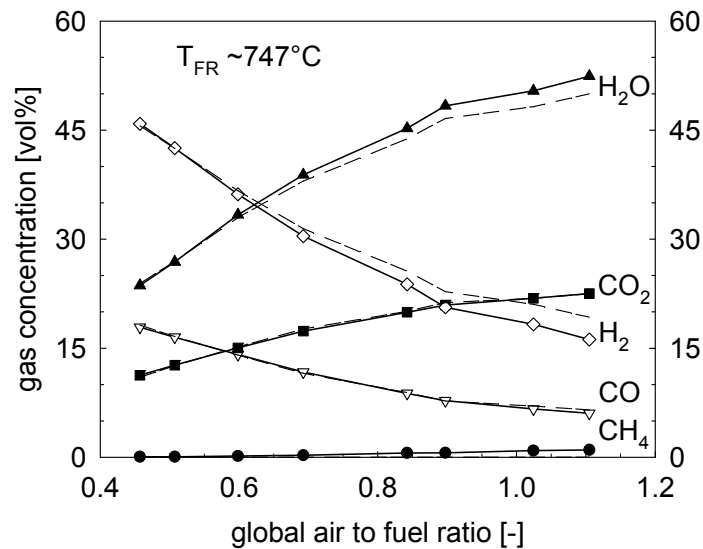


Fig. 26 Wet-gas concentration in the FR exhaust gas at 747°C 140 kW natural gas and S/C =0.4

It is important to notice that no coke formation has been observed at any of the operating points shown in the graphs. From measurement of CO₂ in the AR exhaust gas, exact detection of carbon loss to the AR is possible. These measurements reveal the following:

1. No gas leakage occurs at any time from the FR to the AR (even though system pressure in the bottom region of the FR is higher than in the bottom region of the AR)
2. The onset of coke formation has been found at global air/fuel ratios as low as 0.4 for practically all the temperatures investigated.

The second point represents an unexpected result with respect to the fact that no additional steam is added to the fuel at all. Only the steam from fluidization of the loop seals is present in the FR.

Not only the FR composition but also the oxygen absorption in the AR is an important parameter. It defines the oxygen content transported with the oxygen carrier to the FR. In other words, if in CLR mode oxygen leaves the AR with the gas stream the provided oxygen to the FR does not represent the global air/fuel ratio as defined in Chapter 2.1. To investigate this behavior the oxygen content in the AR exhaust gas is plotted in Fig. 27 for three different FR temperatures. The reactor temperatures represent mean values over the reactor height. With increasing FR temperature a significant increase of the oxygen absorption is observed. The oxygen content reaches the equilibrium oxygen concentration, i.e. no oxygen in the exhaust gas, at an AR temperature of approximately 900°C and a global air/fuel ratio below 1. Only where the oxygen is completely consumed in the AR the global air/fuel ratio describes the actually provided oxygen to the FR. In all other cases less oxygen is actually available in the FR than supplied with the air stream.

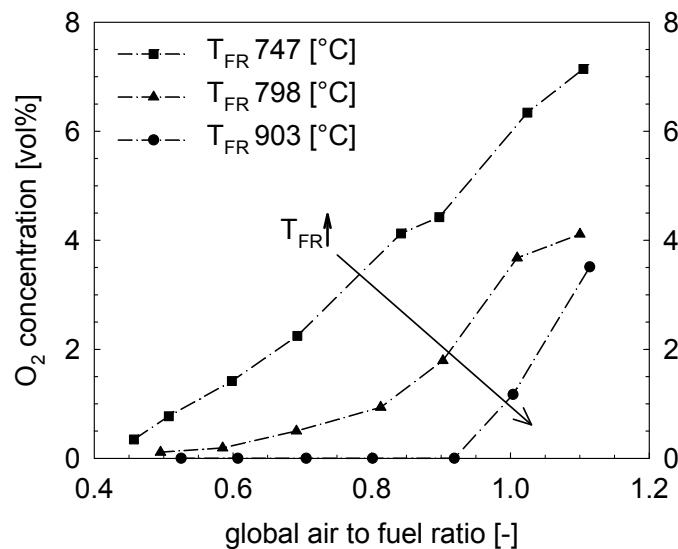


Fig. 27 Oxygen concentration in the AR exhaust gas at three different FR temperatures

In Fig. 28 the AR temperature is shown for the three different constant FR temperatures. The global solids circulation is a strong function of the AR gas velocity, i.e. of the air flow rate introduced in the AR. A temperature difference between AR and FR is necessary to supply the required heat to the FR. Therefore, only one reactor temperature can be kept constant. The AR temperature continuously increases with decreasing global air/fuel ratio. With increasing reactor temperature not only the chemical equilibrium changes but also the reactivity of the oxygen carrier. It is interesting to notice that, independently of the FR temperature, complete oxygen absorption is reached at an AR temperature of approximately 900°C. As a consequence, this temperature value can be regarded as the optimum for full oxygen absorption in the AR with this specific oxygen carrier at a global air/fuel ratio below 1. However, oxygen carrier particles may be further optimized in order to improve oxygen

absorption at lower temperatures. Another point of particle optimization is to decrease the global air/fuel ratio where carbon formation starts to be a problem. A comparison of two different Ni-based oxygen carriers operated at the 120 kW pilot rig has been performed by Kolbitsch et al. [27].

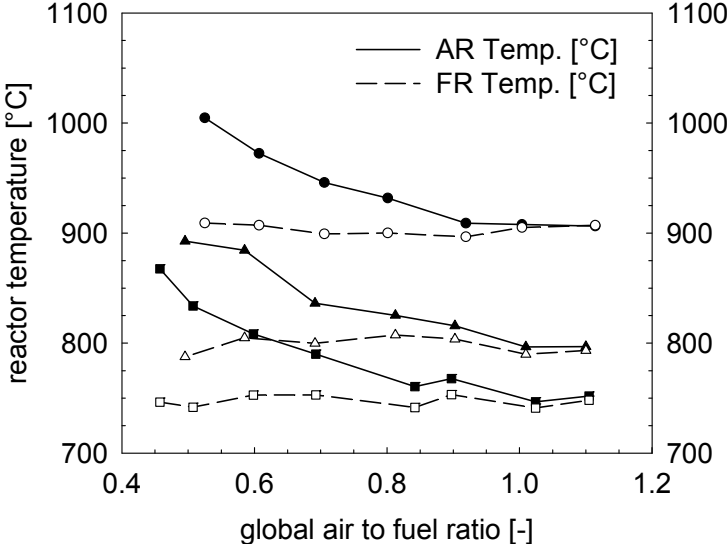


Fig. 28 AR temperature vs. global air/fuel ratio at three different FR temperatures

6

A 10 MW_{TH} CLC CONCEPT

In 2004 first reports were presented from a 10 kW CLC unit operated with gaseous fuels at Chalmers University in Sweden [34, 36], and later in 2004 Ryu et al. [53] reported from a 50 kW CLC unit from the Korean Institute of Energy Research. In January 2008 a 120 kW CLC pilot plant was put into operation at Vienna University of Technology. A detailed description of the plant design can be found in an article and in the PhD thesis by Kolbitsch et al. [26, 28]. Different bed materials were tested under operating condition from CLC to CLR [8, 30, 47].

The next step in process development is to demonstrate this technology in an industrial size application. basic design parameters of a CLC boiler at the scale of 10 MW_{th} were calculated by Lyngfelt et al. [35] in 2001. The design criteria were chosen for an atmospheric circulating fluidized bed (CFB) boiler with a bubbling bed as FR in the return loop of the CFB. The boiler concept assumed in the paper by Lyngfelt et al. [35] to demonstrate CLC technology with gaseous fuel is used for heat production, district heating, or production of industrial process steam.

The proposed 10 MW_{th} CLC boiler is designed for power generation based on the dual circulating fluidized bed (DCFB) design of the 120 kW pilot rig.

The dual circulating fluidized bed (DCFB) boiler

The basic assumptions for the boiler parameters and design are based on the experience and up scaling potential of the 120 kW pilot rig. Fig. 17 represents a possible reactor design. The nominal power of the boiler has been chosen to be 10 MW_{th} with natural gas as the fuel. The most important design values are summarized in Table 10.

Table 10 Chosen or assumed parameter values

Item	Value	Unit
Power (fuel) ~40MJ/kg	10	MW
Heat loss (reactor system)	2	%
AR cross section	1.6	m ²
AR pressure drop	7	kPa
FR cross section	0.75	m ²
FR temperature	900	°C
FR pressure drop	14.5	kPa
Global air/fuel ratio	1.1	–
Solid conversion difference	10	%
Mean AR oxidation state	50	%

The OC, a highly active carrier particle, is based on NiO, α -Al₂O₃, and MgO. The particle size of the oxygen carrier is in the range of 90 to 210 μ m. This OC represents an actual particle operated for several 100 h in three different test rigs [32]. The oxygen carrier characteristics are summarized in Table 11. Additional information on the oxygen carriers used can be found elsewhere [23].

Table 11 Oxygen carrier characterization

Item	Value	Unit
Oxygen carrier system	Ni/NiO	–
Support materials	Al ₂ O ₃ + MgO	–
NiO content	41.3	wt%
d _p	90–210	μ m

The values of Table 10 and Table 11 together with the CL reactor model implemented in the software IPSEpro give the basis for process simulation.

To compare the chemical looping system with a standard air combustion boiler, the combustion efficiency η_{comb} is introduced. The combustion efficiency indicates the ability to burn fuel and is calculated from the amount of unburned fuel in the exhaust gas. In air combustors, excess oxygen in the combustion zone guarantees efficient fuel conversion. In a CLC system only the oxygen needed for the reactions in the FR is actually released in the FR. Therefore no gaseous excess oxygen is available in the FR in any case. Equation (25) describes the combustion efficiency based on the lower heating value of inlet and outlet gas of the FR. The sensible heat of the gas streams is not represented in this definition.

$$\eta_{comb} = 1 - \frac{LHV_{FR, exhaust} \cdot \dot{V}_{FR, exhaust}}{LHV_{FR, fuel} \cdot \dot{V}_{FR, fuel}} \quad (25)$$

The combustion efficiency has its maximum at approximately 0.99 for an Ni-based oxygen carrier, as thermodynamic constraints limit total fuel conversion. In an ideal system, that is full conversion of the fuel and a thermodynamic equilibrium condition for CO and H₂ reactions (Eqs. (26) and (27)), the maximum combustion efficiency is influenced only by temperature.



Different oxygen carriers have different thermodynamic equilibrium gas compositions after combustion. Fig. 14 shows the minimum CO and H₂ concentrations in the FR at a temperature of

850°C for four different oxygen carrier systems. The Ni-based carrier proposed for the CLC boiler application, assuming full CH₄ conversion, reaches equilibrium at a CO wet gas concentration of 0.24 vol-% and at 0.44 vol-% H₂ at 850°C.

The combustion efficiency derived from the experimental data is influenced additionally by the reaction time, the gas-solids mixing, the oxygen carrier conversion rate, the design of the combustion zone, the amount of oxygen carrier, and the fuel composition. Fig. 29 shows a temperature variation at a global air/fuel ratio of 1.1 and at a fuel load of 140 kW. The oxygen carrier used is based on Ni as described in Table 11. Two curves are plotted in Fig. 29 representing the ideal $\eta_{comb, max}$ and the actual combustion efficiency η_{comb} . An increase in combustion efficiency with increasing temperature can be observed. It is most likely that with increasing temperature an increase in the oxygen carrier activity has a beneficial impact on the combustion efficiency. In contrast the ideal combustion efficiency increases slightly with decreasing temperatures to 0.994 at 800 °C. This can be explained by changes in the thermodynamic equilibrium gas concentration.

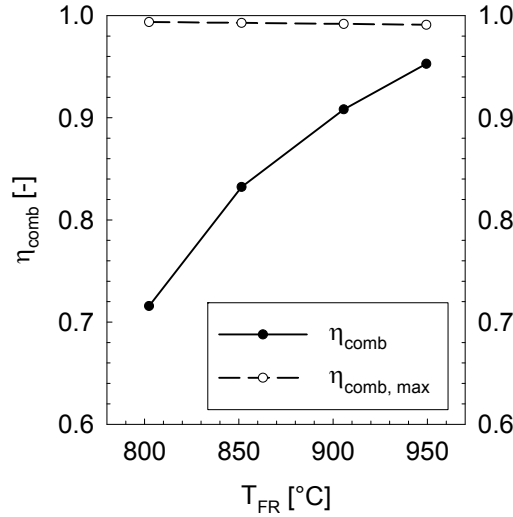


Fig. 29 Combustion efficiency η_{comb} and ideal combustion efficiency $\eta_{comb, max}$

The global air/fuel ratio is a comprehensive parameter for air combustion. It describes the amount of oxygen available for combustion. In CL systems air and fuel are never mixed, and therefore a new parameter ω_{FR} is introduced. ω_{FR} describes the ratio of oxygen actually released from the OC in the FR to the amount of oxygen stoichiometrically needed for complete combustion. Equation (28) defines

$$\omega_{FR} = \frac{O_{2, actually\ released}}{O_{2, total\ combustion}} \quad (28)$$

In contrast to the global air/fuel ratio, ω_{FR} cannot exceed 1. Additional thermodynamic constraints of used oxygen carrier, as described above, limit the ratio in an ideal system to below 1. The dashed line in Fig. 30 shows the maximum ω_{FR} for an Ni-based oxygen carrier for different temperatures. From

measured data, ω_{FR} is derived. The presented data represent a CLC experiment at a global air/fuel ratio of 1.1 with a thermal input of 140 kW of natural gas. The oxygen conversion shows an increase with increasing temperature. For an AR temperature of approximately 950°C, an oxygen conversion of 0.95 is reached.

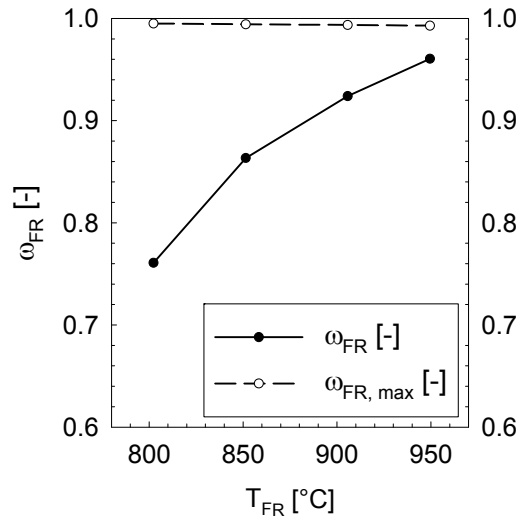


Fig. 30 Oxygen conversion ω_{FR} and ideal oxygen conversion $\omega_{FR, max}$

It can be concluded that the combustion efficiency η_{comb} as well as ω_{FR} increase with increasing temperature. The temperature increase has a limitation due to different constraints. One limiting parameter is the maximum operating temperature of the oxygen carrier, which is determined by agglomerate formation due to sintering or melting. Other parameters in the reactors, for example the solids distribution, influence the presented parameters. It should be noted that the results are only valid for the presented reactor system configuration in combination with the OC used and care must be taken when transferring the results to other reactor concepts or OC particles. Additional work in evaluating the existing data will result in a better understanding of the complex dependencies.

Flow sheet simulation of the 10 MW_{th} CLC boiler for power generation

The software IPSEpro, as described above, offers an open structure for implementation of new process layouts. The AET-Lib enables the user to simulate the CL environment as well as the steam cycle section. In the following a predictive simulation of a CLC boiler for power production is carried out. The basic setup can be seen in the IPSEpro flow sheet shown in Fig. 31. Such a boiler is suitable for semi-commercial demonstration of CLC technology for gaseous fuels. At this scale a simple heat recovery setup is proposed. The steam cycle parameters (live steam parameters, efficiencies) can be found in Table 12.

Table 12 Steam cycle parameters

Item	Value	Unit
Steam temperature	520	°C
Steam turbine inlet pressure	60	bar(a)
Condenser pressure	0.1	bar(a)
Total steam turbine efficiency	89.4	%
Generator efficiency	97.5	%
Pump efficiency	70	%
Motor drive efficiency	90	%
Cooling water inlet temperature	15	°C
Cooling water outlet temperature	25	°C

The process flow diagram in Fig. 31 represents the entire CLC plant without CO₂ compression. The input streams fuel, air, and fresh bed material as well as the output streams AR exhaust, FR exhaust (i.e. CO₂ and H₂O), condensed water, and used bed material are the system boundaries of the plant. Air is provided at ambient pressure and is preheated with heat from the AR exhaust gas whereas the fuel is available at elevated pressure and ambient temperature.

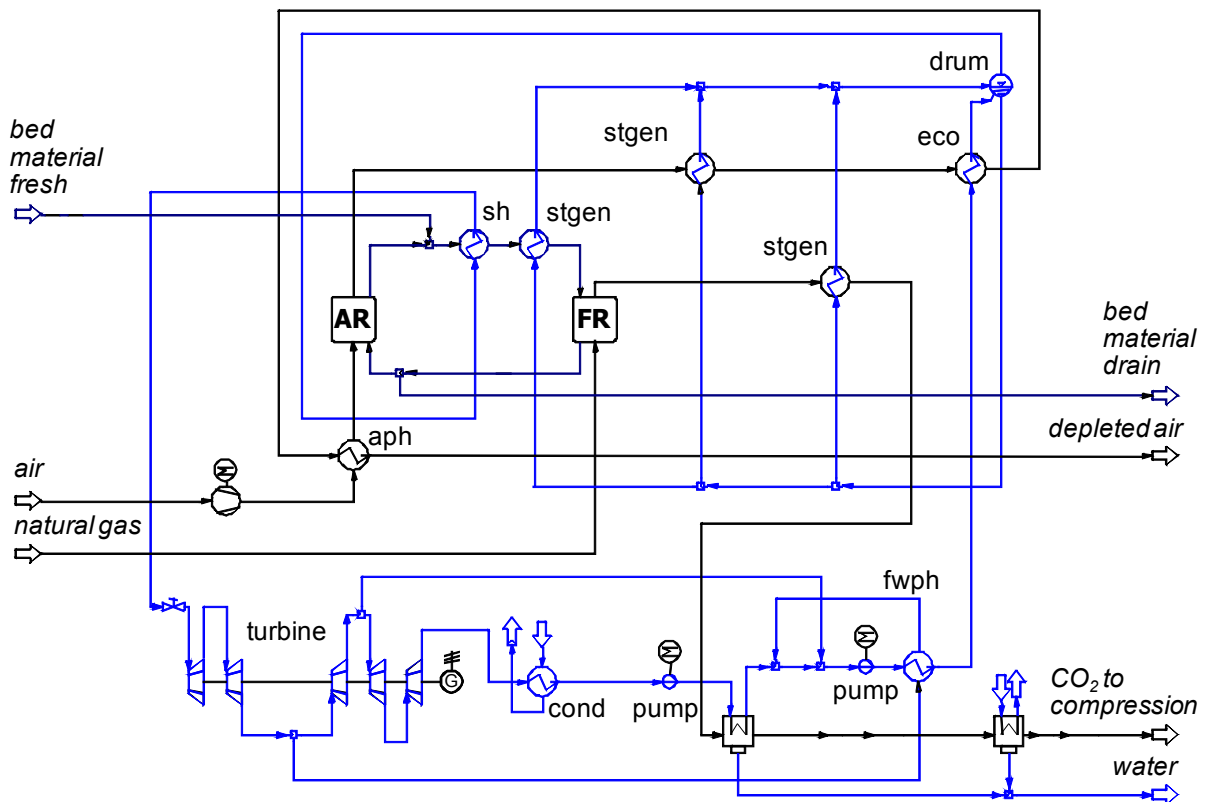


Fig. 31 Basic setup of a chemical looping combustor for power production (aph: air preheater; eco: economizer; fwph: feed water preheater; sh: superheater; stgen: steam generator).

Therefore, only a gas compressor for air is needed. The fuel is taken from the natural gas grid and mainly consists of methane. The IPSEpro simulation covers the CLC boiler, the heat recovery steam generator, and the integrated steam cycle with a steam turbine for power generation. A single pressure steam cycle in natural circulation with no reheat and live steam parameters of 520°C at 60 bar(a) is designed. The steam turbine is divided into five stages with bleed steam connections for feed-water heating and deaeration of the condensed water. The setup of the heat recovery steam generator includes the AR and FR heat recovery boiler and a fluidized bed heat exchanger (FB-HE). The proposed AR heat recovery boiler consists of a steam generator, an economizer, and an air preheater. The components of the AR exhaust gas are N₂ and unreacted O₂, and thus the risk of corrosion is very low. Therefore, it seems feasible to recover heat from the AR exhaust stream down to 60°C.

The heat of the FR exhaust gas is withdrawn by a steam generator. Some of the heat recovered in a FR exhaust gas condenser is used to preheat low temperature feed water. In order to reduce the dew point to 25°C, however, some cooling water is required. At the operating parameters chosen (see Table 10), the amount of heat produced in the reactors is greater than the sensible heat in the exhaust gas streams. Therefore, a FB-HE has to be arranged. This FB-HE consists of two parts: a super heater and a steam generator. The FB-HE is arranged where the heated solids leave the AR.

Discussion of the results

A 10 MW_{th} CLC boiler with heat recovery and a single pressure steam cycle is successfully simulated. The assumed parameters are conservative and CLC reactor parameters are based on the experience of the 120 kW pilot plant [8, 30, 47]. Different basic design parameters are derived from the flow sheet simulation and presented. The bed material inventory in the two reactors is calculated. The turbulent regime in the FR enhances gas–solid contact and thus allows a reduction in the solids inventory [15]. This is one of the advantages of a DCFB concept that is especially relevant at increased plant capacities. The necessary mass in the FR per MW thermal input decreases from 510 kg/MW to 110 kg/MW [28].

The AR has a solid inventory of 1140 kg and is in the same range as in the concept of Lyngfelt et al. [35]. It is important to note that the bed mass in the loop seal and the FB-HE is not considered. The solid circulation rate G_s of 57.1 kg/m²s corresponds to the solid conversion difference of 10% and is in the typical range for CFB risers. According to Smolders and Baeyens [54], G_s can reach values up to 100 kg/m²s in CFB systems. The energy consumption of all auxiliary units is in the range of 1% of the thermal input. The overall net electric efficiency of the 10 MW_{th} CLC power plant is 36.3%. With respect to the semi-commercial scale of the plant this efficiency value may be acceptable; however, more work is needed to assess the potential. The main results of the process flow sheet simulation are summarized in Table 13.

Table 13 Parameter values derived from simulation and the basic assumptions

Item	Value	Unit
Fuel flow	0.28	Nm ³ /s
Air flow	2.87	Nm ³ /s
FR superficial velocity	4.8	m/s
AR superficial velocity	7.3	m/s
FR bed mass	710	kg
AR bed mass	1140	kg
Solid circulation rate G_s	57.1	kg/(m ² s)
Solid flow from AR	85.6	kg/s
Solid flow to AR	84.8	kg/s
Air fan power	61	kW
Pump power	49	kW
Net electric efficiency	36.3	%

CLC features the principle of a chemical heat pump [49]. The basic principle of a chemical heat pump is to bind chemical energy at a lower temperature to the bed material and then transport it to a second reactor where the chemical energy is released as heat at a higher temperature. This sensible heat is contained partly in the exhaust gas of the reactor and partly in the returning bed material. The Sankey diagram in Fig. 32 shows this principle for a CLC boiler with a fuel input of 10 MW_{th}.

The total energy transported by the gas streams is based on the specific sensible enthalpy and lower heating value. For clear illustration of the energy transported by the circulating solids, the following two set points were determined. Firstly, the energy flow from the FR to the AR consists of chemically bound energy only; that is, the sensible heat of the bed material stream at 900°C is set to 0. Secondly, the bed material returning to the FR contains only sensible heat released in the exothermic AR, that is, the chemically bound energy in this energy stream is formally set to 0. This means, in other words, that the sensible heat entering the FR is the difference in sensible heat between the solids streams entering and leaving the FR. Accordingly, the chemically bound energy in the solids stream to the AR is only the difference from the chemically bound energy present in the returning solids stream.

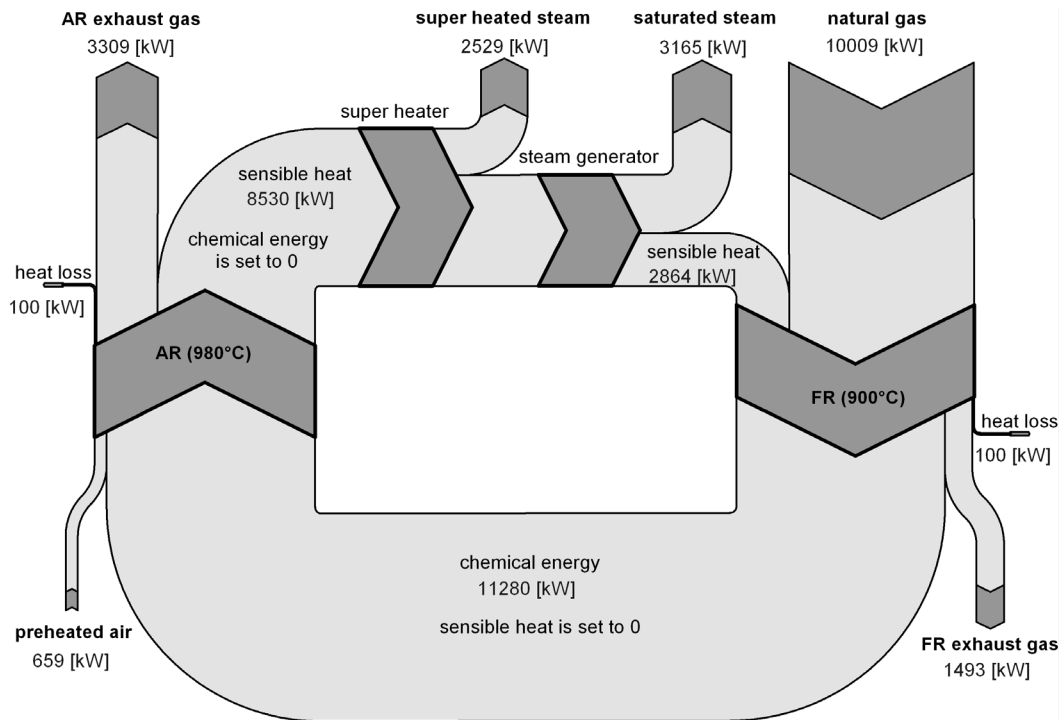


Fig. 32 Energy flows in the 10 MW_{th} CLC boiler

The main energy input in the FR is the natural gas. For the conversion of the fuel, some additional heat is needed as the reaction is slightly endothermic (Ni-based particles). This heat is transported into the FR by returning bed material from the AR. In the FR, the energy input is bound primarily to the outgoing bed material as chemical energy. The smaller part is released with the exhaust gas stream. The bed material transports the chemical energy to the AR where in interaction with the preheated air it is transformed into sensible heat at a higher temperature level (e.g. 980°C). This heat is then released in the exhaust gas stream and in the returning bed material stream. The major part is bound to the bed material. To fulfill the energy balance of the system, heat has to be withdrawn by a FB-HE out of the bed material. The loop is closed by the returning energy flow to the FR.

7

CONCLUSION

The chemical looping system as it is presented in this thesis represents the only technology without a significant energy penalty for sequestration and one of the technologies which can capture 100% CO₂. Therefore, the potential of chemical looping systems as a 2nd generation carbon capture technology is high.

In the design phase a simulation tool was needed for mass- and energy balance calculations of the chemical looping pilot rig. Therefore, a modeling tool for chemical looping based processes based on the conservation laws was created in the IPSEpro simulation environment. This tool includes different solid species and allows optional thermodynamic equilibrium calculation. The comparison of different oxygen carrier redox systems shows that Ni-, Cu-, Fe-, and Mn-based carriers have a high potential for fuel oxidation.

The design of the reactor system, as described in the PhD thesis of Philipp Kolbitsch [26], is a dual circulating fluidized bed system (DCFB) which allows variation of global air/fuel ratio over a wide range without adaptations on the reactor system or at the auxiliary equipment. The thesis comprehends the presentation of the 120 kW chemical looping pilot rig and the successfully demonstration of chemical looping autothermal reforming at atmospheric pressure. For all experimental results high methane conversion is observed determined by gas concentration analysis. Methane conversion reaches thermodynamic equilibrium for all FR temperatures at a global air/fuel ratio below 0.7. All other species run along the equilibrium curves with significant deviations only where methane conversion is incomplete. The maximum H₂/CO ratio in the synthesis gas of 2.6 can be seen at a FR temperature of 747°C. Even though no steam has been added to the fuel apart from the loop seal fluidization (what would result in an steam/carbon ratio of 0.4 for the worst case assumption that all steam from the lower loop seal enters the FR), no coke formation has been observed for global air/fuel ratios above 0.46. Furthermore, the oxygen absorption in the AR was investigated. At an AR mean temperature of approximately 900°C the oxygen absorption reaches equilibrium, below this temperature unreacted oxygen leaves the AR with the exhaust gas.

These experimental results underline the potential of CLR as new concept for reforming systems today. Already in the 1950-ies CLR was invented [31] but it could obviously not compete with fixed bed reforming systems up to now. The major drawbacks are for sure the necessary dust removal from the product streams, difficulties in making dual fluidized bed systems work at attractive conditions (increased pressure) and the need for attrition-resistant catalyst particles. Today, significant progress has been made in basically all of these fields. There are bag filter systems available for operation at increased temperatures up to 250°C, dual fluidized bed systems have been demonstrated at industrial

scale [17] and pressurized circulating fluidized bed combustion systems have been put in operation [11]. The lifetime of the catalyst particles used within this thesis, manufactured from commercially available raw materials, has been calculated to more than 33000 hours under fluidized bed conditions [32]. Considering these achievements together with the advantages of CLR especially with respect to increased operating temperatures in the reformer and reduced reactor volume, CLR may be an attractive competitor to standard reforming technology in the near future.

In addition to the experimental work the setup of the 120 kW pilot rig is simulated in the IPSEpro environment and the measurements of the experiments are used for validation of the model. Due to redundant measurements an over-determined equation system with a redundancy of 10 allows describing the actual plant operation best within the limits of the model structure. The final outcome represents a robust and reliable engineering tool for full size power plant simulation which allows the specification of the main process parameters like solids circulation rate, difference of oxygen carrier conversion between the reactors, heat extraction, etc.

As a next step an integrated power plant layout was investigated to determine the potential of chemical looping combustion (CLC) as CO₂ free technology. Based on a continuous development of the chemical looping technology from laboratory scale to pilot scale, a first basic design for a semi-commercial 10 MW_{th} CLC plant for power production is proposed. The design criteria for the CLC boiler are based on the experience from the 120 kW CLC pilot rig operated more than 400 h. The CLC boiler represents a new circulating fluidized bed reactor concept, which was developed at Vienna University of Technology. This new dual circulating fluidized bed (DCFB) concept is demonstrated in a cold flow model and in the 120 kW pilot rig, as described above. On the basis of successful implementation of the required unit operations, the process flow sheet of a whole power plant has been set up. A single pressure steam cycle with live steam parameters of 520°C and 60 bar is suggested to suit the demonstration plant scale. Heat exchangers are arranged to recover heat from the bed material and exhaust gas streams. A five-stage steam turbine is designed with conservative efficiency estimation. The simulation provides additional design parameters (mass flow, volume flows, velocities, etc.). The net electric efficiency of 36.3% is plausible considering the small scale of the plant. However, more information about the detailed design and about the plant site is needed to assess the potential of such a concept. An alternative to power generation would be an application in the field of industrial steam generation. A natural gas steam generator could be replaced by CLC boiler without any significant drop in efficiency compared to the standard solution. This could already be attractive at a small scale provided that at least a minimum economic benefit results from delivering CO₂ for storage.

8

NOTATION

A	species in reaction
AET-Lib	advanced energy technology library
AR	air reactor
CCS	Carbon capture and storage
CFB	circulating fluidized bed
CL	chemical looping
CLC	chemical looping combustion
CLC-StR	Chemical looping combustion steam reforming
CLR	chemical looping reforming
DCFB	dual circulating fluidized bed
d_p	particle size [μm]
ECBM	enhanced coal bed methane recovery
EGR	enhanced gas recovery
EOR	enhanced oil recovery
FB-HE	fluidized bed heat exchanger
FBH-StR	fluidized bed tubular steam reformer
FCC	fluid catalytic cracking
FR	fuel reactor
GHG	green house gas
G_s	solid circulation rate [$\text{kg}/\text{m}^2 \cdot \text{s}$]
i	index of species
IAPWS-IF97	International Association for the Properties of Water and Steam - Industrial Formulation 1997
IPCC	Intergovernmental Panel on Climate Change
K_p	equilibrium constant [$\text{bar}^{\sum \nu_i}$]
$LHV_{FR, exhaust}$	lower heating value of the fuel reactor exhaust gas
$LHV_{FR, fuel}$	lower heating value of the fuel to the fuel reactor
LOSU	level of scientific understanding
$m_{0, i}$	mass of the sample i [kg]
Me	metal
MeO	metal oxide
\dot{m}_{fuel}	mass flow of the fuel [kg/h]
$\dot{m}_{OC, ox}$	mass flow of the fully oxidized oxygen carrier [kg/h]
m_{ox}	mass of the fully oxidized sample [kg]
m_{red}	mass of the fully reduced sample [kg]
OC	oxygen carrier
O_{min}	oxygen demand of the fuel [kg/kg]
p	partial pressure [bar]

p^*	equilibrium partial pressure [bar]
PSE	process simulation environment
$p\delta_{eq}$	logarithmic deviation from equilibrium
$Q_{cooling}$	cooling duty [kW]
Q_{loss}	heat loss of the pilot rig [kW]
R	universal gas constant [J/(mol·K)]
RF	Radiative forcing
R_0	Oxygen transport capacity [kg/kg]
$R_{0,i}$	Particle oxygen transport capacity [kg/kg]
T	temperature [K]
T_{melt}	melting temperature [°C]
tol_{x_i}	tolerance of the measurement value x_i
UNFCCC	United Nations Framework Convention on Climate Change
$\dot{V}_{FR, exhaust}$	volume flow of the fuel reactor exhaust gas [m ³ /h]
$\dot{V}_{FR, fuel}$	volume flow of the fuel to fuel reactor [m ³ /h]
\bar{x}_i	mean value of the measurement
x_i	value of the measurement
X_S	solids conversion
ΔG_R^0	Gibbs free enthalpy of reaction [J/mol]
$\Delta\Omega$	mass fraction difference
Ω_i	mass fraction of the solid sample i
η_{comb}	combustion efficiency
ν	stoichiometric factor
ω_{FR}	oxygen conversion in the air reactor

9

REFERENCES

- [1] ABAD, A., ADANEZ, J., GARCIA-LABIANO, F., DE DIEGO, L. F., GAYAN, P., AND CELAYA, J. Mapping of the range of operational conditions for Cu-, Fe-, and Ni-based oxygen carriers in chemical-looping combustion. *Chemical Engineering Science* 62, 1-2 (2007), 533–549.
- [2] ABAD, A., MATTISSON, T., LYNGFELT, A., AND JOHANSSON, M. The use of iron oxide as oxygen carrier in a chemical-looping reactor. *Fuel* 86, 7-8 (2007), 1021–1035.
- [3] ABANADES, J. C., ANTHONY, E. J., LU, D. Y., SALVADOR, C., AND ALVAREZ, D. Capture of CO₂ from combustion gases in a fluidized bed of CaO. *AIChE Journal* 50, 7 (July 2004), 1614–1622.
- [4] ANDRUS, H. Chemical looping combustion - R&D efforts by Alstom. In *Proceedings of the IEA GHG 2nd Workshop of the International Oxy-Combustion Research Network* (Windsor, USA, 2007).
- [5] ANDRUS, H. E., CHIU, J. H., LILJEDAHL, G. N., STROMBERG, P. T., THIBEAULT, P. R., AND JAIN, S. C. ALSTOMs hybrid combustion-gasification chemical looping technology development - phase II. In *Proceedings of the 23rd Annual International Pittsburgh Coal Conference* (Pittsburgh, PA, USA, September 25 - 28 2006), pp. 20–.
- [6] BARIN, I. *Thermochemical Data of Pure Substances*. VCH-Verl.-Ges., Weinheim, 2004.
- [7] BASU, P., AND FRASER, S. A. *Circulating Fluidized Bed Boilers - design and operations*. Butterworth-Heinemann, 1991.
- [8] BOLHAR-NORDENKAMPF, J., PRÖLL, T., KOLBITSCH, P., AND HOFBAUER, H. Performance of a NiO-based oxygen carrier for chemical looping combustion and reforming in a 120 kW unit. *Energy Procedia* 1, 1 (February 2009), 19–25.
- [9] BURCAT, A., AND MCBRIDE, B. *1997 ideal gas thermodynamic data for combustion and air-pollution use*. Technion Israel Institute of Technology, Haifa, 1997.
- [10] CORBELLA, B. M., AND PALACIOS, J. M. Titania-supported iron oxide as oxygen carrier for chemical-looping combustion of methane. *Fuel* 86, 1-2 (2007), 113–122.
- [11] DODD, A. M., DRYDEN, R. J., AND MOREHEAD, H. T. McIntosh Unit 4 PCFB Demonstration Project. In *Proceedings of the American Power Conference* (Chicago, Illinois, USA, April 1997), pp. 562–567.
- [12] DYBKJAER, I. Tubular reforming and autothermal reforming of natural gas – an overview of available processes. *Fuel Processing Technology* 42, 2-3 (1995), 85–107. Trends in Natural Gas Utilisation.

- [13] FLORIN, N. H., AND HARRIS, A. T. Enhanced hydrogen production from biomass with in situ carbon dioxide capture using calcium oxide sorbents. *Chemical Engineering Science* 63 (2008), 287–316.
- [14] GARCIA-LABIANO, F., ADANEZ, J., DE DIEGO, L. F., GAYAN, P., AND ABAD, A. Effect of pressure on the behavior of copper-, iron-, and nickel-based oxygen carriers for chemical-looping combustion. *Energy & Fuels* 20, 1 (2006), 26–33.
- [15] GRACE, J. R. High-velocity fluidized bed reactors. *Chemical Engineering Science* 45, 8 (1990), 1953–1966.
- [16] HOFBAUER, H., RAUCH, R., BOSCH, K., KOCH, R., AND AICHERNIG, C. The Biomass CHP plant guessing - a success story. In *Pyrolysis and Gasification of Biomass and Waste*, A. Bridgwater, Ed. CPL Press, Newbury, UK, 2003, pp. 527–536.
- [17] HOFBAUER, H., RAUCH, R., LOEFFLER, G., KAISER, S., FERCHER, E., AND TREMMEL, H. Six years experience with the FICFB-Gasification process. In *Proceedings of the 12th European Conference on Biomass and Bioenergy* (Amsterdam, The Netherlands, June 2002), Eigenverlag, p. 4.
- [18] HUGI, E., AND REH, L. Design of cyclones with high solids entrance loads. *Chemical Engineering & Technology* 21, 9 (1998), 716–719.
- [19] IPCC. *Special Report on Carbon Dioxide Capture and Storage*. Cambridge University Press, Cambridge, United Kingdom and New York, NY, USA, 2005. Prepared by Working Group III of the Intergovernmental Panel on Climate Change.
- [20] IPCC. *Climate Change 2007: Synthesis Report*. IPCC, Geneva, Switzerland, 2007.
- [21] ISHIDA, M., AND JIN, H. A new advanced power-generation system using chemical-looping combustion. *Energy* 19, 4 (1994), 415–422.
- [22] ISHIDA, M., ZHENG, D., AND AKEHATA, T. Evaluation of a chemical-looping-combustion power-generation system by graphic exergy analysis. *Energy* 12, 2 (1987), 147–154.
- [23] JERNDAL, E., THIJS, I., SNIJKERS, F., MATTISSON, T., AND LYNGFELT, A. NiO particles with Ca and Mg based additives produced by spray-drying as oxygen carriers for chemical-looping combustion. *accepted for publication in Energy Procedia* (2008).
- [24] JOHANSSON, M., MATTISSON, T., AND LYNGFELT, A. Use of NiO/NiAl₂O₄ particles in a 10 kW chemical-looping combustor. *Industrial & Engineering Chemistry Research* 45, 17 (2006), 5911–5919.
- [25] JUKKOLA, G., LIJEDAHL, G., NSAKALA, N. Y., MORIN, J., AND ANDRUS, H. An Alstom vision of future CFB technology based power plant concepts. In *Proceedings of the 18th International Conference on Fluidized Bed Combustion* (Toronto, ON, Canada, May 22-25 2005), ASME, pp. 109–120.

- [26] KOLBITSCH, P. *Chemical looping combustion for 100% carbon capture - Design, operation and modeling of a 120 kW pilot rig*. PhD thesis, Vienna University of Technology, 1060 Wien, Austria, January 2009.
- [27] KOLBITSCH, P., BOLHAR-NORDENKAMPF, J., PRÖLL, T., AND HOFBAUER, H. Comparison of two Ni-based oxygen carriers for chemical looping combustion of natural gas in 140 kW continuous looping operation. *Accepted for publication in Industrial & Engineering Chemistry Research* (2009).
- [28] KOLBITSCH, P., BOLHAR-NORDENKAMPF, J., PRÖLL, T., AND HOFBAUER, H. Design of a chemical looping combustor using a dual circulating fluidized bed (DCFB) reactor system. *Chemical Engineering and Technology* 32, 3 (2009), 398–403.
- [29] KOLBITSCH, P., PRÖLL, T., BOLHAR-NORDENKAMPF, J., AND HOFBAUER, H. Characterization of chemical looping pilot plant performance via experimental determination of solids conversion. *Energy & Fuels* 23, 3 (2009), 1450–1455.
- [30] KOLBITSCH, P., PRÖLL, T., BOLHAR-NORDENKAMPF, J., AND HOFBAUER, H. Operating experience with chemical looping combustion in a 120 kW dual circulating fluidized bed (DCFB) unit. *Energy Procedia* 1, 1 (February 2009), 1465–1472.
- [31] LEWIS, W. K., AND GILLILAND, E. R. Production of pure carbon dioxide. U.S. Patent Office, Number 2,665,972, 1954.
- [32] LINDERHOLM, C., MATTISSON, T., AND LYNGFELT, A. Long-term integrity testing of spray-dried particles in a 10-kw chemical-looping combustor using natural gas as fuel. *Fuel In Press* (2009).
- [33] LYNGFELT, A., JOHANSSON, M., AND MATTISSON, T. Chemical-looping combustion - status and development. In *Proceedings of the 9th International Conference on Circulating Fluidized Beds* (2008), pp. 39–53.
- [34] LYNGFELT, A., KRONBERGER, B., ADANEZ, J., MORIN, J.-X., AND HURST, P. The GRACE project: Development of oxygen carrier particles for chemical-looping combustion. Design and operation of a 10 kW chemical-looping combustor. In *Proceedings of the 7th Conference on Greenhouse Gas Control Technologies* (Vancouver, Canada, 2004), pp. –.
- [35] LYNGFELT, A., LECKNER, B., AND MATTISSON, T. A fluidized-bed combustion process with inherent CO₂ separation; application of chemical-looping combustion. *Chemical Engineering Science* 56, 10 (2001), 3101–3113.
- [36] LYNGFELT, A., AND THUNMAN, H. Construction and 100h of operational experience of a 10-kW chemical looping combustor. In *Carbon Dioxide Capture for Storage in Deep Geologic Formations*. Elsevier Science, Amsterdam, 2005, ch. 31, pp. 625–645.
- [37] LYON, R. K., AND COLE, J. A. Unmixed combustion: An alternative to fire. *Combustion & Flame* 121 (2000), 249–261.

- [38] MARX, K. Potential of hydrogen and power generation from natural gas with quantitative carbon capture using chemical looping technology. Master's thesis, Vienna University of Technology, Wien, Austria, April 2009.
- [39] MATTISSON, T., JOHANSSON, M., AND LYNGFELT, A. The use of NiO as an oxygen carrier in chemical-looping combustion. *Fuel* 85, 5-6 (2006), 736–747.
- [40] PAISLEY, M., FARRIS, M., BLACK, J., IRVING, J., AND R.P., O. Preliminary operating results from the battelle/FERCO gasification demonstration plant in Burlington, Vermont, USA. In *Proceedings of the 1st World Conference on Biomass for Energy and Industry* (Sevilla, Spain, 2000).
- [41] PERZ, E. A computer method for thermal power cycle calculation. *Journal of Engineering for Gas Turbines and Power* 113, 2 (1991), 184–189.
- [42] PRÖLL, T., BOLHAR-NORDENKAMPF, J., KOLBITSCH, P., MARX, K., AND HOFBAUER, H. Pure hydrogen and pure carbon dioxide from gaseous hydrocarbons by chemical looping reforming. In *Proceedings of the 2009 AIChE Spring National Meeting and 5th Global Congress on Process Safety* (Tampa, FL, USA, April 2009).
- [43] PRÖLL, T., AND HOFBAUER, H. Development and application of a simulation tool for biomass gasification based processes. *International Journal of Chemical Reactor Engineering* 6, A89 (2008), –.
- [44] PRÖLL, T., AND HOFBAUER, H. H₂ rich syngas by selective CO₂ removal from biomass gasification in a dual fluidized bed system – Process modeling approach. *Fuel Processing Technology* 89, 11 (2008), 1207 – 1217.
- [45] PRÖLL, T., KOLBITSCH, P., BOLHAR-NORDENKAMPF, J., AND HOFBAUER, H. Fluidized bed reactor system. International Application No.: PCT / AT2008/000287, February 2009. Pub. No.: WO/2009/021258.
- [46] PRÖLL, T., KOLBITSCH, P., BOLHAR-NORDENKAMPF, J., AND HOFBAUER, H. A novel dual circulating fluidized bed (DCFB) system for chemical looping processes. *accepted for publication in AIChE Journal* (2009).
- [47] PRÖLL, T., MAYER, K., BOLHAR-NORDENKAMPF, J., KOLBITSCH, P., MATTISSON, T., LYNGFELT, A., AND HOFBAUER, H. Natural minerals as oxygen carriers for chemical looping combustion in a dual circulating fluidized bed system. *Energy Procedia* 1, 1 (February 2009), 27–34.
- [48] PRÖLL, T., RUPANOVITS, K., KOLBITSCH, P., BOLHAR-NORDENKAMPF, J., AND HOFBAUER, H. Cold flow model study on a dual circulating fluidized bed (DCFB) system for chemical looping processes. *Chemical Engineering and Technology* 32, 3 (2009), 418–424.
- [49] RICHTER, H. J., AND KNOCHE, K. F. Reversibility of combustion processes. *ACS Symposium Series* 235 (1983), 71–85.

- [50] RYDEN, M., AND LYNGFELT, A. Hydrogen and power production with integrated carbon dioxide capture by chemical-looping reforming. In *Proceedings of the 7th Conference on Greenhouse Gas Control Technologies* (Vancouver, Canada, 2004).
- [51] RYDEN, M., AND LYNGFELT, A. Using steam reforming to produce hydrogen with carbon dioxide capture by chemical-looping combustion. *International Journal of Hydrogen Energy* 31 (2006), 1271–1283.
- [52] RYU, H., BAE, D., AND JIN, G. Chemical-looping combustion process with inherent CO₂ separation; reaction kinetics of oxygen carrier particles and 50kWth reactor design. In *The World Congress of Korean and Korean Ethnic Scientists and Engineers, Seoul, Korea* (2002), pp. 738–743.
- [53] RYU, H., JIN, G., AND YI, C. Demonstration of inherent CO₂ separation and no NO_x emission in a 50 kW chemical-looping combustor: Continuous reduction and oxidation experiment. In *Proceedings of the 7th Conference on Greenhouse Gas Control Technologies (GHGT-7)* (Vancouver, Canada, 2004).
- [54] SMOLDERS, K., AND BAEYENS, J. Gas fluidized beds operating at high velocities: a critical review of occurring regimes. *Powder Technology* 119, 2-3 (2001), 269–291.
- [55] SON, S. R., AND KIM, S. D. Chemical-looping combustion with NiO and Fe₂O₃ in a thermobalance and circulating fluidized bed reactor with double loops. *Industrial & Engineering Chemistry Research* 45, 8 (2006), 2689–2696.
- [56] STRATMANN, K. Ministerien verständigen sich auf Gesetz zur Kohlendioxidspeicherung. *Handelsblatt Düsseldorf* 250 (February 2009), 4.
- [57] UNFCCC. *Kyoto protocol reference manual on accounting of emission and assigned amount*. No. ISBN 92-9219-055-5. United Nations Framework Convention on Climate Change, 2008.
- [58] U.S. DEPARTMENT OF ENERGY. *Carbon sequestration technology roadmap and program plan*. 2007.
- [59] VAN DER DRIFT, B., VAN REE, R., BOERRIGTER, H., AND HEMMES, K. Bio-syngas: Key intermediate for large scale production of green fuels and chemicals. In *Proceedings of the 2nd World Conference on Biomass for Energy, Industry and Climate Protection* (Rome, Italy, May 2004), vol. II, pp. 2155–2157.
- [60] WAGNER, W., AND KRUSE, A. *Properties of water and steam: the industrial standard IAPWS-IF97 for the thermodynamic properties and supplementary equations for other properties: tables based on these equations*. Springer-Verlag, Berlin, New York, 1998.

Curriculum Vitae

DI Johannes Bolhar-Nordenkamp

Beethovengang 10
1190 Wien

m 0699/10 33 33 36
e: johannes.bolhar@gmx.at



Persönliche Daten

Geburtsdatum, -ort: 20. Juni 1979, Villach
Staatsbürgerschaft: Österreich
Familienstand: ledig
Wehrdienst: abgeleistet (September 1998 –Mai 1999)

Ausbildung

2005 – heute Doktorat der Technischen Wissenschaften auf dem Gebiet der Verfahrenstechnik
(Schwerpunkt Wirbelschichttechnik, Energietechnik)
1999 – 2005 Studium an der TU WIEN, Wirtschaftsingenieurwesen-Maschinenbau
Abschluss mit Diplomingenieur
1998 Abschluss der AHS mit Matura
1991 – 1998 AHS Wien IX, Wasagasse mit Aufenthalt in Australien

Sprachen

Deutsch: Muttersprache
Englisch: fließend
Französisch: Grundkenntnisse
Spanisch: Grundkenntnisse

Berufserfahrung

Seit 2005 – heute fixes Anstellungsverhältnis am Institut für Verfahrenstechnik als
Projektassistent auf dem Gebiet der Wirbelschichtverbrennung
2000, 2001 und 2004 je ein Monat bei Opel Austria PowerTrain
in der Produktionsleitung (siehe Zeugnis im Anhang)
1998, 1999, und 2001 jeweils ein Monat bei der Firma Stahlbau Ing. Preinl
als Schlossergehilfe (siehe Zeugnis im Anhang)

Zusatzqualifikationen

Führerschein: Führerschein der Klassen A, B, C, E
PC-Kenntnisse (Microsoft Office; AutoCad, Catia, IPSEpro Simulation, Visio, SPS
Programmierung B&R)

Freizeitinteressen

Laufen, Basketball, Schifahren, Lesen, Motorrad fahren, Tauchen, Reisen

Wien, April 09